scientific reports

Check for updates

OPEN

Enhancing the power quality of dual rotor wind turbines using improved fuzzy space vector modulation and super twisting sliding techniques

Habib Benbouhenni[1]✉, Nicu Bizon[2,3], Mourad Yessef[4], Z. M. S. Elbarbary[5,6], Ilhami Colak[7], Mohammed M. Alammar[5,6] & Badre Bossoufi[4]

In the field of control, many approaches have been used to control generators, where indirect vector control (IVC) is considered one of the most prominent of these approaches due to its many advantages. This approach has a fast response time (RT) and is quite easy to realize. However, its reliance on traditional controllers makes this approach less efficient and less effective if the system parameters change. Consequently, this work proposes a new IVC approach for doubly-fed induction generators (DFIG) used in contra-rotating wind turbine (CRWT) systems. The designed IVC employs a super-twisting control to eliminate the instantaneous errors of the DFIG power using the direct calculation of the control voltage required by the rotor, which will lead to the improvement of the transient performance. In addition, a constant switching frequency is obtained using the multilevel fuzzy modified space vector modulation proposed for controlling the DFIG inverter, facilitating the design of harmonic AC filters. To evaluate the proposed solution, a digital simulation of the CRWT system was verified using MATLAB with the power of the used generator being 1.5 MW. For more accuracy, two tests were used to study the efficiency of the suggested control compared to the efficiency of the IVC in terms of getting better system features. The obtained results showed the efficacy of the designed control compared to the IVC and some of the different existing techniques in terms of enhancing system features. The suggested approach minimized torque fluctuations, active power, and current in the first test compared to the IVC approach by ratios estimated at 93%, 97%, and 98%, respectively. Also, the RT for reactive power, active power, and torque was reduced by 99.05%, 98.60%, and 98.60%, respectively, compared to the conventional IVC approach. In both tests, the designed approach minimized the harmonic distortion of the stream by ratios estimated at 18.02% and 16.22% compared to the conventional IVC approach. These obtained results were verified using empirical work, where hardware-in-the-loop simulation was used for this purpose. Accordingly, the empirical results demonstrated the validity, durability, and competence of the designed approach compared to the base IVC approach. Both the simulative and empirical results validate that the designed approach is of great importance in the field of control and renewable powers, as it can be relied upon to enhance the features of the systems. Therefore, the designed control has a promising future.

Keywords Super-twisting sliding mode control, Multilevel fuzzy simplified space vector modulation, Indirect vector control, Contra-rotating wind power turbine systems, Doubly-fed induction generator

[1]Laboratoire LAAS, Ecole Nationale Polytechnique d'Oran, Bp 1523, EL M'naouer, Algeria. [2]The National University of Science and Technology POLITEHNICA Bucharest, Pitești University Centre, 110040 Pitesti, Romania. [3]ICSI Energy, National Research and Development Institute for Cryogenic and Isotopic Technologies, 240050 Ramnicu Valcea, Romania. [4]LIMAS Laboratory, Faculty of Sciences, University of Sidi Mohamed Ben Abdallah, Fes, Morocco. [5]Department of Electrical Engineering, College of Engineering, King Khalid University, P.O. Box 394, 61421 Abha, Saudi Arabia. [6]Center for Engineering and Technology Innovations, King Khalid University, 61421 Abha, Saudi Arabia. [7]Istinye University, Istanbul, Turkey. ✉email: habib.benbouhenni@enp-oran.dz

Renewable energies (REs) are in continuous development as a result of reliance on them to decrease the emission of toxic gases and overcome the problem of the increasing demand for electrical energy (EE)[1]. REs contribute significantly to global energy production, as they have many and varied advantages that qualify them to be the most desired source of generating EE and an effective solution for non-petroleum countries. Using these sources allows reducing the bill for producing and importing EE. Solar energy, wind energy (WE), potential hydropower, wave energy, and ocean currents are among the most prominent RE sources currently relied upon to generate EE[2]. WE is one of the types of REs on which researchers have focused a lot in the field of EE generation, as it relies on the use of turbines called wind turbines (WTs) to transfer WE into mechanical power (MP). The latter is used to rotate the generator and thus generate electric current[3]. Because of its cleanliness, ease, profitability, and non-exhaustion, the WE has become one of the most important and promising techniques in the future.

In fact, this RE respects the environment and helps to reduce carbon dioxide significantly, as the use of these clean energies inevitably leads to a diminution in dependence on conventional sources that produce toxic gases. As it is known, toxic gases are undesirable because they help pollute the atmosphere and raise the temperature of the atmosphere[4]. One of the downsides of toxic gases in the atmosphere is that it helps in dehydration and chronic diseases.

In the field of WE, WTs are one of the most essential elements of the WE system, as they have received great interest from all researchers to enhance the EE quality gained from WE and raise its value. These WTs can be divided into two main branches, and each branch has advantages and disadvantages. The first kind is fixed-speed WTs (FSWTs)[5] and the second kind is variable-speed WTs (VSWTs)[6]. But, the VSWT is more used in WE compared to the FSWT system. Several scientific studies have concluded that operating at a variable-speed allows extracting more energy from the wind compared to using an FSWT[7]. This is what is observed in recent times, the heavy reliance on VSWTs in the establishment of WT farms and the generation of stream. According to the work done in[8], WTs can be classified into vertical-axis WTs and vertical-axis WTs. The difference between the two types lies in the energy yield obtained, ease of control, cost, ease of maintenance, and ease of implementation on the ground. Horizontal axis WTs are considered the most widespread on land and at sea compared to the other type[9]. In[10], a novel WT has emerged under the name multi-rotor WT to replace traditional WTs in producing EE. These WTs are described by high efficacy and great robustness compared to usual WTs, as their use leads to a significant augment in the MP gained from the WE[11]. Also, the use of these WTs overcomes the WE generated between the WTs in the WE farm, which allows increasing the yield of WE farms.

To generate EE from VSWTs, several generators can be used. Among these generators, most popular ones are induction generator (IG)[12], doubly-fed IG (DFIG)[13], wound rotor synchronous generator, squirrel cage IG, and permanent magnet synchronous generator (PMSG)[14]. The DFIG is the largely used and researched in the field of the VSWTs, due to their many and varied characteristics. The latter can be summed up in easy to control, robustness, it features minimum energy loss, efficiency, low cost, and less maintenance[15]. In addition, these generators can operate at a speed that varies by 33% around the synchronous speed[16]. To obtain a high-power quality created from DFIG, several control techniques are used. Among these techniques, direct power control (DPC)[17], super-twisting algorithm[18], sliding mode control (SMC)[19], backstepping control (BC)[20], fuzzy logic (FL) control[21], field-oriented control (FOC)[22], direct torque control (DTC)[23], terminal synergetic control (SC)[24], and hybrid control[25–29] are very popular techniques. In power systems (PSs) that rely on WE, the quality of the resulting EE is one of the most famous drawbacks that hinder the spread of these PSs. Also, the resulting EE is largely linked to the wind speed (WS) profile, which causes disturbances in energy production in difficult natural conditions, leading to unwanted problems at the network level. So the choice of the type of control used is important, as the control approach has an important role in improving power quality. So, it is necessary to choose a suitable controller with high performance, great efficacy, and high durability. Recently, many researchers have developed and proposed new controls based on combining controls with the aim of obtaining a new control with high features.

Vector control (VC) is one of the largest and most used techniques in AC machines because it is a simple approach[30]. This approach uses a traditional proportional-integral (PI) type regulator to control the feature quantities, which makes it have a simple structure that offers a fast dynamic response (DR)[31]. Also, this approach uses pulse width modulation (PWM) to run the machine's inverter, making it experimentally easy and inexpensive to implement. This approach was used to control several equipment, including interior permanent magnet (PM) synchronous motors[32], DFIG[33], PMSG[34], PMSM[35,36], and three-phase PM motors[37]. There are two kinds of VC techniques which are as follows: direct VC (DVC)[38] and indirect VC (IVC)[39], where they differ in terms of the difficulty, the results obtained, the degree of vulnerability to the change of DFIG parameters, and the number of controls used to control the distinct quantities. The IVC approach is rather complicated compared to the DVC. Using the VC approach in the field of controlling electrical machines (EMs) has several problems, as it presents larger ripples of stream and torque. Also, durability decreases if machine parameters change. This approach provided unsatisfactory results compared to both DTC and FS-MPC techniques presented in[40]. According to the work[41], the IVC approach is one of the reliable approaches for controlling EMs due to its fast DR and ease of experimental realization. Compared to DTC or DPC, the IVC approach provides lower power and current quality when using DFIG, as there is a significant impact if the DFIG parameters change. This effect appears significantly in the high fluctuations of power, stream, and torque. Also, a significant increase in the value of total harmonic distortion (THD) of current. All of these drawbacks limit the spread of this type of control in the field of REs.

Several works have suggested a new technique for IVC using artificial intelligence. In[42], IVC was suggested based on a neuro-FL technique to regulate the DFIG-WT energy. In this paper, the neuro-FL algorithm was used to replace traditional PI controllers, because its use allows a significant augment in competence and robustness, as demonstrated by simulation results. However, the drawback of energy fineness remains an issue, especially in the event of a change in the machine's parameters, as a noticeable augment in power ripples is observed in the

robustness test. In[43], the use of type 2 FL (T2FL) was designed to enhance the IVC performance of DFIG. The T2FL approach was used to replace usual regulators, as the resulting approach is described by high robustness and distinguished performance in terms of minimizing EE fluctuations and the stream THD compared to IVC of DFIG and this is shown by the results in all tests. However, the use of the T2FL approach leads to an augment in the degree of complexity by using a larger number of gains and therefore difficulty in its implementation. However, it is worth noting that the number of rules is adequate for the T2FL approach to achieve good results as if a larger number of rules is used, the PS becomes heavier, which is not desirable. Neural networks (NNs) were used as a suitable solution to defeat the shortcomings of the IVC approach of DFIG in[44], where classical controllers were dispensed with and replaced with other neural-type controllers. NN-IVC is simple and easy to implement, effective in reducing current ripple and THD value, and with high robustness and fast DR. This approach was confirmed using MATLAB, and the results showed the high efficacy of the NN-IVC approach compared to the baseline IVC-PI approach. Despite this good competence, stream and energy ripples are still present and they increase noticeably, especially in the robustness test, which is a negative matter that makes the search for the best reliable approach continue to obtain high fineness energy in the event of a fault in the PS.

There are those who believe that nonlinear approaches are among the best solutions that can be relied upon to overcome the problems of the IVC approach. In[45], the IVC was suggested based on adaptive BC-SMC of the DFIG-based contra-rotating WT (CRWT). The use of the adaptive BC-SMC led to ameliorating the problems and defects of the IVC largely, and this is shown by the value of stream THD and energy ripple compared to the IVC-PI.

The super-twisting SMC (STSM) is a nonlinear method that has been popularized recently in the field of generator regulation. In recent years, they have been used more in RE due to some advantages like low dependency on the machine parameters, more simplicity, and robust control. The STSM approach was introduced in 1999 by Utkin et al.[46], especially for nonlinear PSs. This regulator does not need the model of AC machines; moreover, the STSM regulator is not sensitive to parameter variations compared to the classical controller such as PI controllers or hysteresis controllers (HCs). In the STSM approach, the output signal from the STSM is comparable with the control signal realized from conventional PI[47]. In[48], the authors proposed the use of the DPC with STSM approaches for DFIG. In this proposed approach, HCs were dispensed with and replaced with an STSM, and SVM (Space vector modulation) was used instead of the switching table (ST). The use of the STSM greatly improved the drawbacks of the DPC, especially in the case of changing the DFIG parameters. However, the DPC-STSM is described by its ease of realization, simplicity, and high solidity. Also, there are always ripples in current and energy. It was proposed to improve the effectiveness of the SMC approach based on the use of the STSM strategy to control the DC microgrid[49]. In this proposed strategy, the switching rule of the conventional sliding mode control has been changed by adding super twisting control law. The proposed approach is characterized by high performance and great robustness, which differs from the traditional approach. This proposed strategy ensures the stability of the system during steady state and ensures that the output voltage remains constant whether the input voltage changes or the load power is constant. The performance of the proposed controller is verified through both simulations in MATLAB/Simulink and experimental studies. The obtained results showed that the proposed strategy significantly reduced the effect of chatter, which is the biggest drawback of sliding mode control. The disadvantage of the proposed approach lies in its complexity, which increases the difficulty of completion and costs, which is undesirable. In[50], the robustness of the photovoltaic (PV) system was enhanced by using the STSM regulators. In this work, the STSM approach was used to enhance the features of the maximum power point tracking (MPPT) approach of PV. The STSM-MPPT approach is a simple, effective, robust approach, and has effective performance compared to the MPPT, and this is what the results show. However, despite the outstanding performance of STSM-MPPT, the drawback of EE fluctuations remains, and this negativity can be attributed to the choice of STSM-MPPT parameters. In[51], a PMSM command based on STSM regulators has been designed. The use of the STSM to control the PMSM led to an enhancement in the DR, and this is shown by the response time (RT) to torque and speed compared to the PI control. The use of the STSM controller makes the control PS not affected much by the change of machine parameters, and this is a good thing indicating the high ability of the STSM controller. STSM was designed to control the DC machine[52], as using this approach does not require complex calculations or large costs. The designed control is simple, efficient, and has a low gain number which makes adjusting the DR easier. This designed approach was experimentally realized using dSPACE 1104, with results compared to the usual approach. Experimental results showed that using STSM significantly improved DC machine performance. However, the drawback of torque and stream fluctuations remains present, as it is observed that there are fluctuations at the level of torque and stream. In[53], the efficiency of the interior PMSM was enhanced by using the STSM. The use of the STSM to control the interior PMSM significantly overcame the drawbacks of the PI control such as torque fluctuations and response time (RT). Another approach for STSM was proposed in[54], where this approach is NN-STSM. The NN-STSM approach is a combination of NN and STSM, where NNs were used as a suitable solution to augment the robustness and performance of the STSM approach. This designed approach was applied to the DPC of DFIG, where HC was compensated with NN-STSM type controllers and ST was compensated using the PWM approach. The DPC-NN-STSM approach is different from the DPC in terms of performance, efficiency, robustness, and effectiveness. But the same estimation equations are used as in the DPC. This approach was realized using MATLAB, where variable WS profile was used. All test results prove the higher efficacy of the DPC-NN-STSM compared to the DPC and this is shown by minimizing the stream THD, overshoot, steady-state error (SSE), and ripples of EE. Despite this performance, in the robustness test, it is noted that this designed approach was greatly affected due to its reliance on power estimation. This effect appears significantly in high fluctuation values, overshoot, SSE, and stream THD. The STSM approach was used in[55] as a suitable solution to augment the competence of the direct FOC approach of the multi-phase induction motor (MPIM). The suggested approach is the development of FOC-PI, where all PI controllers are replaced with STSM-type controllers. The

use of STSM allows for a significant augment in robustness and performance. But using STSM increases the number of gains and complexity compared to using PI. The designed approach, FOC-STSM, was realized using MATLAB and experimentally, where dSPACE 1104 was used to verify the approach experimentally under different working conditions. The FOC-STSM approach provided better results than FOC-PI, and this is confirmed by the simulation and experimental results. The proposed approach has the disadvantages of complexity, experimental cost, and unsatisfactory DR compared to FOC-PI. Also, the drawback of torque and stream fluctuations remains present, causing a problem for the PS, as this negativity can be attributed to not using smart approaches to estimate the gains of the designed control. The[56] presents a development control to enhance the efficiency of the DC bus voltage loop regulation in a WE converter system driven by DFIG, where, the STSM is based on a metaheuristics control approach. It has been proven through this work that the combination of non-linear controls and intelligent controls is of great importance in improving current accuracy and is considered one of the best reliable solutions that can be relied upon in the field of regulating EMs. In[57], it is proposed to use thermal exchange optimization-based STSM to enhance the robustness and reduce the cons of the DPC used for controlling DFIG. The latter is present in the generation PS that uses a single-rotor WT. The suggested approach in this work is described by robustness and its ability to enhance the stream quality and minimize fluctuations significantly compared to the IVC.DPC based on a second-order SMC (SOSMC) controller is a different approach from the DPC in terms of competence, robustness, control idea, ease of realization, number of gains, and DR. This designed approach uses the same power estimation equations found in DPC. MATLAB was used to realize this approach, where a variable WS profile was used to study the performance and compare the results with DPC. All test results show the advantage of this approach over DPC, and this is demonstrated by the graphical results and the stream THD. Despite this superiority, the problem of power fluctuations remains, which is a negative matter due to the use of power estimation. Also, there are a significant number of gains that make DR adjustment difficult, even if smart approaches are used to determine them[58]. The STSM and the FL method were combined to control the horizontal-axis WT with DFIG feeding directly from the mains in the stator and using two converters, one on the stator side (SGC) and another on the rotor side (RSC)[59,60]. The FL-STSM approach is described by high competence and great robustness compared to the STSM approach and PI control, which was used to control the RSC. Note that the outputs of the FL-STSM approach are voltage reference values (VRVs) which are then converted to pulses using the PWM approach. MATLAB was used to realize the FL-STSM approach using a variable WS profile to study the efficiency and effectiveness compared to traditional control. All test results highlight the high competence of the FL-STSM approach, and this is demonstrated by the minimization of energy fluctuations and the stream THD. The use of the FL-STSM approach has many disadvantages since the use of this approach requires the estimation of powers, which makes them affected if the DFIG parameters change. Also, it is noted that ripples remain present at the energy and stream levels, which is negative. There is also no mathematical rule that facilitates the use of the FL approach in choosing the best number of rules to obtain good results, which makes it difficult to obtain strong control. The FL-STSM approach has a significant number of gains, which makes it difficult to adjust the DR value easily. All these drawbacks limit the spread of this control in the field of control. In[61], particle swarm optimization (PSO) was used to increase the solidity of the STSM. This intelligent approach is used to estimate the parameters of the STSM to adjust the optimal response. The PSO-STSM approach is easy, inexpensive, and easy to realize, and applying it to PSs does not require precise information about the mathematical model (MM). This designed approach was realized using MATLAB and was compared with the traditional approach. The results presented showed that using this approach led to a significant enhancement and increase in energy quality. But the problem of gossip still exists, as it has not been eliminated. In the robustness test, it is noted that this designed approach was significantly affected by changing PS parameters, which is negative. In[62], an NN-STSM is developed for a DFIG-WT. The designed intelligent nonlinear regulator is composed of recurrent high-order NN trained with the Extended Kalman Filter, which is used to build-up the DFIG models. The suggested control proved its high ability to significantly enhance the PS response, especially in terms of RT and fluctuations. Also, this approach is described by high efficacy and ease of application. The voltage-oriented control was developed based on the STSM to control the DFIG energy for a variable-speed and fixed-pitch WE conversion system with a DFIG[63]. The control objective is to maximize the total *Ps* delivered by the PS at the meanwhile regulating the *Qs* of the converters. The cons of this approach are that it is somewhat complex and affected by the change in PS parameters. Moreover, it is highly related to the MM of the PS under study and this is not desirable. An adaptive super-twisting multivariable fast terminal SMC based on time delay estimation and asymmetric error constraints is suggested to guarantee high-precision trajectory tracking control of cable-driven manipulators under complicated unknown uncertainties[64]. This designed approach differs from the usual approach, as it is described by high robustness and the ability to significantly enhance PSs. Its use allows for increasing the competence, efficiency, and robustness of PSs. However, this approach has some disadvantages, such as the presence of a significant number of gains and high complexity, which makes experimental implementation difficult and expensive. The control PS is constrained by joint position errors, which are asymmetric and time-varying. This approach was realized using MATLAB, with results compared to the traditional approach. The results presented showed the high competence and the extent of its efficacy in getting better the features of the studied PS.

A new form of STSM approach has been designed to enhance the EE quality[65]. This approach was called simplified STSM (SSTSM), because was described by simplicity, thus ease of realization. The SSTSM approach is a simplified and illustrated image of the STSM approach. This presented approach is characterized by a small number of gains, fast DR, and ease of realization, and its use does not require MM knowledge of the PS, which makes it an effective solution in complex systems. This approach was used to control energies, and two regulators were used for this purpose. Using SSTSM requires power estimation, as its outputs are VRVs. These values were used to generate control pulses in the RSC. MATLAB was used to realize the SSTSM approach and compare it with the usual approach, where a variable WS profile was used to complete this work. The test results highlight

the advantage of the SSTSM approach over the usual approach in terms of robustness and performance. Also, in terms of reducing energy fluctuations and the stream THD. In[66], a comparative study was conducted between the STSM and back-stepping controller, where the author relied on digital simulation to accomplish this comparison by using a DFIG-based WT. This comparison was implemented in MATLAB after comparing the two approaches, where a variable WS was used to complete this study. Simulation results show that back-stepping controller leads to superior performance and improved transient response compared to the STSM controller. Another comparative study between STSM and SMC approaches was conducted in[67] to show which approach has the best ability to get better the power quality generated by DFIG. First, an MM was given for each approach, mentioning the pros and cons. These two approaches were used to control power, and they were applied to RSC only. MATLAB was used to implement both the SMC and STSM approaches, where variable WS was used. All the tests performed showed that STSM provided good results in terms of RT, EE fineness, SSE, and undershoot compared to SMC. Also, the STSM approach minimized the chatter value significantly compared to the SMC. These results make STSM a reliable solution in the field of REs. In[68], the author gave another MM of STSM under the name of modified STSM (MSTSM), where this approach is completely different from the STSM approach. MSTSM is described by high efficacy, ease of realization, inexpensiveness, simplicity, and few gains. Also, using this proposed approach does not require MM knowledge of the PS, which makes it easy to apply. This approach was used to defeat the cons of applying DPC to DFIGs through proper power control. MSTSM outputs are VRVs, and these values are converted by PWM into pulses to operate the RSC only. GSC was used by an uncontrolled inverter to simplify the PS and demonstrate the ability of the designed control to get better power quality without resorting to GSC. The DPC-MSTSM approach was verified using MATLAB with results compared to the classical approach. According to the results obtained, the power quality is high when using the DPC-MSTSM approach. However, using this approach has drawbacks, as higher ripples are observed in the robustness test due to the use of EE estimation. Also, the DPC-MSTSM approach provided a greater time for capabilities than the DPC approach, which is a negative. In[69], the adaptive STSM approach was relied upon to control a DC motor, where the difficulty of driving the angular position of a DC servo motor system with atypical wide backlash nonlinearity was demonstrated. The designed approach was verified experimentally using real equipment, and the results were compared with both PI and STSM. Empirical results show that the suggested technique has high efficacy compared to both PI and STSM. In[70], the author used the STSM controller to estimate the speed and acceleration of a remotely operated system, where only the location measurement was relied upon. In[71], the author used the STSM approach and fractional-order PI algorithms respectively to control the generation system using a large power generator (1500 kW). FO-PI-STSM is a new approach with high robustness and great ability to enhance system features, which were relied upon in this work for power control of DFIG. In addition to using the FO-PI-STSM, PWM was used to create the pulses needed to work the RSC. The gains of the FO-PI-STSM approach were calculated using the PSO algorithm, as using this algorithm allows for augment incompetence and an effective reduction in EE fluctuations and the THD value of stream. The FO-PI-STSM was realized using MATLAB and compared to the classical PI-based approach. All results highlight the superiority of the FO-PI-STSM in getting better the features of the studied PS. The RSC and GSC of a 2000 kW DFIG-WT were designed using a non-linear, strong, rattling super-twisting terminal sliding-order SMC (STTSOSMC)[72]. The STTSOSMC approach is a development and modification of STSM, where a terminal sliding surface is used to increase competence and robustness. The STTSOSMC approach was used to control the power and enhance the performance of the GSC. The STTSOSMC approach is distinguished from STSM by several advantages, complexity, and difficulty of realization. However, its use led to getting better the features of the studied PS in terms of power fineness and minimizing the value of THD of stream, and this is shown by the results. Also, using STTSOSMC improved the features of the DC link voltage, which is a good thing. In addition to the complexity, the use of the STTSOSMC approach is based on the use of power estimation, which makes it provide unsatisfactory results if the generator parameters change. In[73], a novel control for the STSM called the modified STSM and uses this technique to control DFIG is suggested. Compared to the STSM approach, the modified STSM is of medium complexity and contains more parameters, which makes it difficult to adjust the DR of the systems. Also, the designed control proved its worth in ameliorating the results of the generation system in terms of EE fluctuations and RT compared to both STSM and SMC.

When scanning the literature and observing the above-mentioned works, the control strategy plays an important role in improving the power quality and the THD value of the current. Also, the robustness of the control strategy used plays an important role in improving the performance of the control PS. The degree of complexity and ease of application and completion must be focused on, as the degree of complexity plays an important role in reducing costs and facilitating the implementation of the PS experimentally. Energy ripples and high THD values are among the most prominent drawbacks found in PSs that use renewable sources. Therefore, this work proposes an effective and appropriate solution to overcome these problems. In this work, it is proposed to use the IVC strategy based on STSMC to control the power of the DFIG-CRWT system. The IVC-STSMC strategy is an upgraded strategy of the IVC approach and is proposed to reduce the power and torque ripples for DFIG-CRWT. Also, reduce the THD of current. Therefore, the IVC-STSMC approach is considered the first main contribution of this paper. This proposed approach uses four STSMC controllers, and these controllers are used to determine VRVs. This proposed strategy is used to control the operation of the RSC of DFIG-CRWT only. For good operation and high performance of the RSC, it was proposed to use the five-level fuzzy modified SVM (FMSVM) strategy to generate the necessary pulses. These pulses are generated from the reference voltage values generated by the STSMC controller. The use of the five-level FMSVM strategy in this paper is the second major contribution of this paper. This proposed strategy is different from the traditional SVM strategy in terms of performance and effectiveness. The use of this strategy, along with the use of IVC-STSMC, makes the work different from the work mentioned above and of great importance in the energy field. Also, the use of a CRWT turbine makes the completed work highly valuable compared to the existing work.

CRWT is a new type of turbine that has recently emerged as an alternative solution to raise the energy gained from wind and as an alternative solution to using traditional turbines. Therefore, the use of CRWT turbines is the third major contribution of this paper.

In this work, the IVC-STSMC approach, which uses the five-level FMSVM strategy, is first implemented in MATLAB using two different WS profiles, comparing the results with both the traditional approach and some works in terms of power ripples, RT, overshoot, and SSE of DFIG power. The simulation results in all tests showed the high performance of the IVC-STSMC approach based on the five-level FMSVM strategy in terms of improving power quality and reducing the value of THD of current. Second, the proposed approach is implemented experimentally using hardware-in-the-loop (HIL) using dSPACE 1104 card while comparing the performance with the traditional approach. Therefore, the implementation of the proposed approach in HIL testing is considered the fourth main contribution of this paper. Implementing the designed approach in the HIL test gives a clear picture of the validity and safety of the designed approach and its experimental implementation, as the experimental results demonstrated the validity of the simulation results and the effectiveness of the proposed approach in improving the quality of power and current compared to the traditional approach. These obtained results highlight the effectiveness, efficiency, and high performance of the IVC-STSMC approach based on the five-level FMSVM strategy compared to the traditional approach and some works, as demonstrated by the completed comparison, which makes it a promising solution that can be relied upon in the future in other industrial applications. Therefore, the objectives achieved in this paper can be summarized in the following points:

- The simulation results confirm the effectiveness and safety of the experimentally designed approach;
- Overcoming the disadvantages of the traditional IVC approach;
- Improving the DR of DFIG-CRWT power;
- Significantly increasing the robustness of the traditional control strategy;
- Significantly improves the IVC-PI robustness;
- Minimized THD compared to the IVC-PI;
- Reduced values of SSE and undershoot compared to IVC-PI.

This paper is prepared as follows. "Materials and methods" section presents the CRWT model, the MM of the STSM regulator, the designed multilevel FMSVM technique, the IVC-PI, and the designed IVC approach. In "Results" and "Discussion", sections the results using the MATLAB are analyzed and presented. The experimental results obtained from the HIL test for the two controls are listed in "Experimental results" section. After all, "Conclusions" section concludes the study by presenting the main findings and future directions of research, as well as some recommendations and comments.

Materials and methods

The designed approach can be clarified by a simple scheme through which the necessary stages for its implementation are explained. Figure 1 represents the diagram of the stages of modeling, design, implementation, and validation of IVC-STSM-FMSVM. The next subsections will detail the dynamic modeling of the CRWT system, the MM of the STSM, the multilevel MSVM technique, and the designed multilevel FMSVM technique.

CRWT system model

The use of the WECS has amplified significantly in recent years. The applied PSs of WT systems can be classified into VSWTs and FSWTs. The VSWTs are now more often applied than the PSs with FST. The main positives of VSWTs are: raising the fabrication of WE, the ability to attain maximum energy conversion effectiveness, and the minimization of mechanical stresses[74]. The use of turbines in wind farms is affected by the wind generated between the WTs, which reduces the yield of the wind farm. The use of traditional WTs is greatly affected by strong winds, which increases losses and costs. In order to obtain greater energy, giant wind turbines with large dimensions must be used. The use of giant WTs increases the difficulty and costs of implementing wind farms, allowing the costs of energy production and consumption to rise. All these disadvantages limit the spread and use of WTs in the field of electric power generation. Therefore, researchers developed WTs to overcome existing defects and problems. One of the solutions that have been proposed to reduce turbine dimensions and overcome problems is the use of multi-rotor WTs. Among the most famous types of multi-rotor WTs, the CRWT can be mentioned. The CRWT is a new technology of WT to overcome the cons of the conventional WTs. This WT has been proposed to obtain more power from WE[75]. The use of a CRWT turbine allows for reducing the area of wind farms and thus reducing the costs of implementing wind farms. Also, using this WT allows reducing the size of the turbine, which leads to the completion of the WT with ease and without difficulties. In case of strong winds, the use of CRWT has greater resistance compared to conventional WTs, allowing for reducing losses and maintenance costs. However, it has a large number of mechanical components compared to classic WTs. According to the work done in[76], CRWT is more difficult to control than conventional WTs. CRWT is also considered more expensive than conventional WTs because it is a new technology and is still in constant development. Figure 2 represents an EP generation system using a CRWT. By observing this figure, it can be said that this system is completely similar to the classic system for generating energy, and the difference lies in the type of WT used. As it is known, the purpose of using a CRWT is to obtain more ME from the WE. On the other hand, this proposed new technology is detailed in[76–78]. However, this technology is a combination of two WTs in the same WT, or in another way, a small WT has been added to the original WT. In this way, it is possible to get more energy and mechanical torque. The two WTs have the same axis of rotation, and the torque and power resulting from them can be expressed by the following equations:

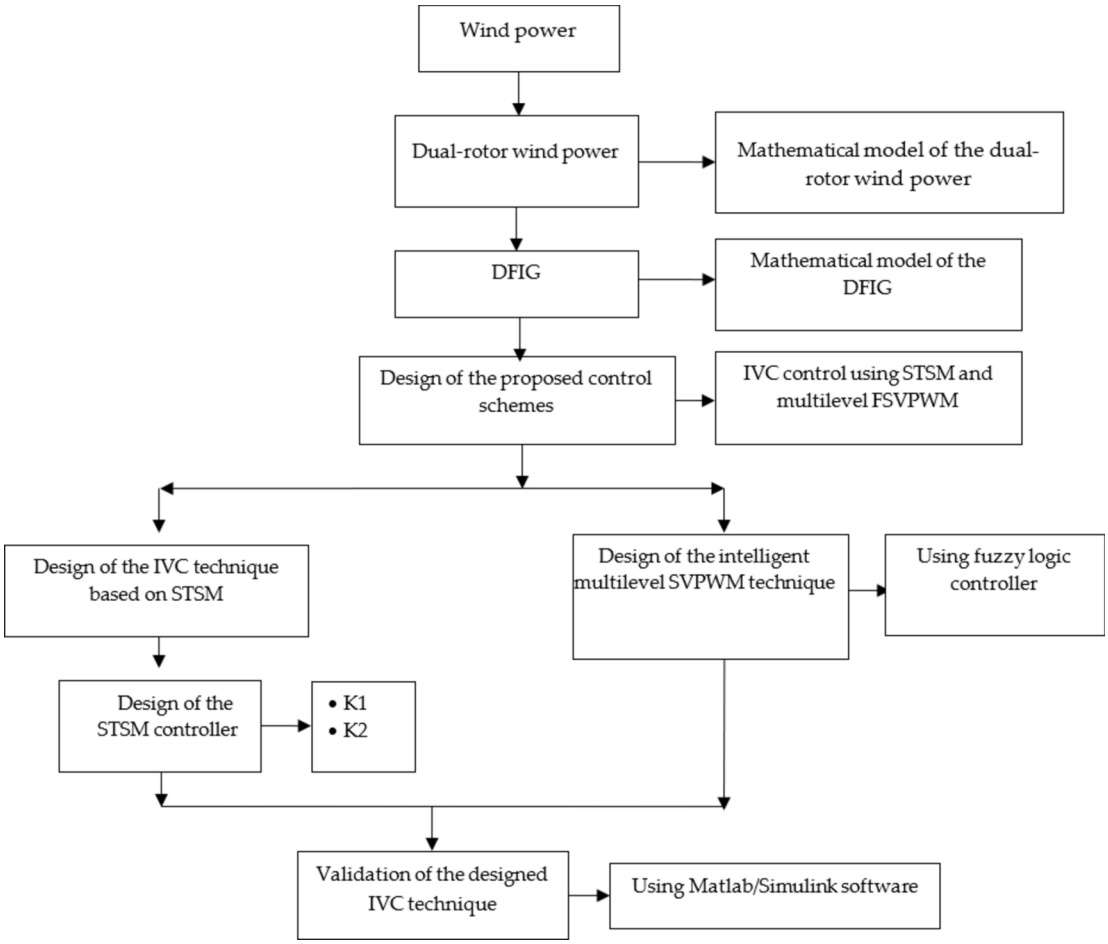

Fig. 1. Chart for suggested IVC control.

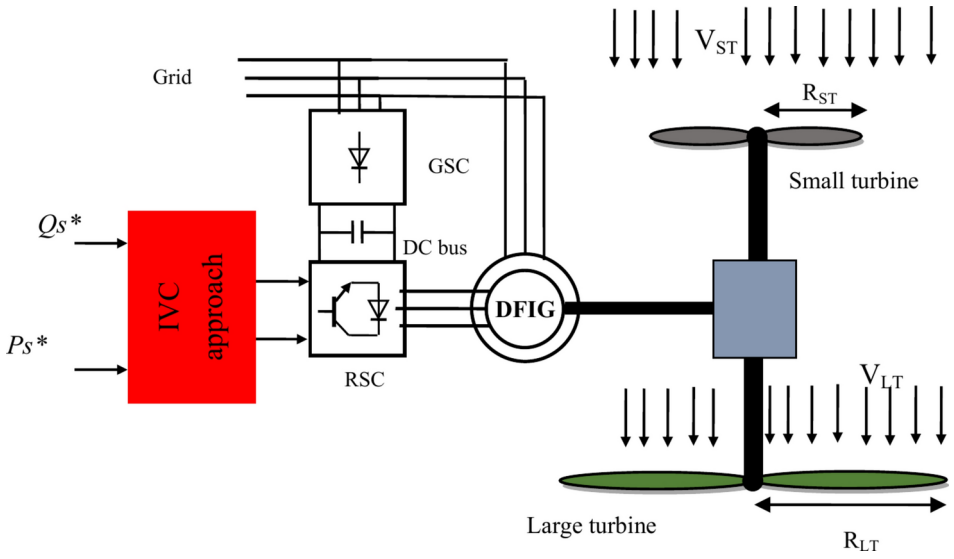

Fig. 2. CRWT system with DFIG.

$$P_{CRWP} = P_T = P_{ST} + P_{LT} \tag{1}$$

$$T_{CRWP} = T_T = T_{ST} + T_{LT} \tag{2}$$

where, T_{LT} and T_{ST} are the output torque of the large and small WTs, P_{LT} and P_{ST} are the output ME of the large and small WT torque.

The torques of a small WT and a large WT can be expressed by Eqs. (3) and (4), respectively.

$$T_{LT} = \frac{C_{pLT}}{2\lambda_{LT}^3}\rho \cdot \pi \cdot R_{LT}^5 \cdot w_{LT}^2 \tag{3}$$

$$T_{ST} = \frac{C_{pST}}{2\lambda_{ST}^3}\rho \cdot \pi \cdot R_{ST}^5 \cdot w_{ST}^2 \tag{4}$$

where ρ is the air density; w_{ST} and w_{LT} are the mechanical speed of the small and large WTs; R_{ST} and R_{LT} are the blade radius of the small and large WTs; λ_{ST} and λ_{LT} are the tip speed ration (TSR) of the small and large WTs.

The *Cp* of large WT is given by:

$$C_{pLT}(\beta, \lambda) = \frac{1}{0.08\beta + \lambda} + \frac{0.035}{\beta^3 + 1} \tag{5}$$

Equations (6) and (7) express the value of the ME generated by the small WT and the large WT, respectively:

$$P_{ST} = \frac{C_{pST}(\beta, \lambda)}{2}\rho \cdot S_{ST} \cdot w_{ST}^3 \tag{6}$$

$$P_{LT} = \frac{C_{pLT}(\beta, \lambda)}{2}\rho \cdot S_{LT} \cdot w_{LT}^3 \tag{7}$$

Equations (8) and (9) express the value of the λ of the small WT and the large WT, respectively:

$$\lambda_{ST} = \frac{w_{ST} \cdot R_{ST}}{V_{ST}} \tag{8}$$

$$\lambda_{LT} = \frac{w_{LT} \cdot R_{LT}}{V_{LT}} \tag{9}$$

where V_{ST} and V_{LT} is the speed of the unified WE on small and large WTs.

WS is the main component used in calculating the TSR. The WS can be calculated at any point between the small and large WTs using the following equation:

$$V_{ST} = V_{LT}\left(1 - \frac{1 - \sqrt{(1 - C_T)}}{2}\left(1 + \frac{2x}{\sqrt{1 + 4x^2}}\right)\right) \tag{10}$$

With *x*: the distance between the small and large WTs, V_{ST} is the WS at a point *x*, C_T is a constant value ($C_T = 0.9$). In this work, this distance between the center of the small and large WT is 15 m[66].

In order to understand the system in a good way, the MM of the generator used to generate EP must also be given. As it is known, DFIG is among the most widely used machines, especially in the CRWT systems due to its robustness. DFIG is considered low-cost compared to other generators and easy to control, making it one of the most suitable and reliable solutions. Also, the use of DFIG does not require regular maintenance, which allows its use to reduce costs. The use of DFIG allows for good control of the output power compared to other generators, as the rotor part is fed to control the output power in the stator part. In the case of using DFIG in PSs, the stator of the DFIG is connected directly to the network without an intermediary, which makes costs lower compared to using a synchronous generator. All these features make DFIG an effective solution in the field of REs, especially in the case of variable WSs.

To find out the MM of DFIG, the Park transform is used. The Park transform is a way to simplify the MM of DFIG. The Park transform is used to give the mathematical equations that represent the rotor and stator of the DFIG. According to the works[35,79], the flux and voltage of the rotor can be written in the Park reference frame using Eqs. (11) and (12).

$$\begin{cases} V_{dr} = R_r I_{dr} - w_r \Psi_{qr} + \frac{d}{dt}\Psi_{dr} \\ V_{qr} = R_r I_{qr} + w_r \Psi_{dr} + \frac{d}{dt}\Psi_{qr} \end{cases} \tag{11}$$

$$\begin{cases} \Psi_{dr} = L_r I_{dr} + M I_{ds} \\ \Psi_{qr} = M I_{qs} + L_r I_{qr} \end{cases} \tag{12}$$

where *M* is the mutual inductance, Ψ_{dr} and Ψ_{qr} are the rotor fluxes, V_{dr} and V_{qr} are the rotor voltages, L_r is the inductance of the rotor, I_{dr} and I_{qr} are the rotor streams, R_r is the rotor resistance.

Stator voltage and flux components:

$$\begin{cases} V_{qs} = R_s I_{qs} + w_s \Psi_{ds} + \frac{d}{dt}\Psi_{qs} \\ V_{ds} = R_s I_{ds} - w_s \Psi_{qs} + \frac{d}{dt}\Psi_{sd} \end{cases} \tag{13}$$

$$\begin{cases} \Psi_{qs} = M I_{qr} + L_s I_{qs} \\ \Psi_{ds} = L_s I_{ds} + M I_{dr} \end{cases} \tag{14}$$

Torque is given by the following relationship:

$$T_e = 1.5p\frac{M}{L_s}\left(-\Psi_{sd} I_{rq} + \Psi_{sq} I_{rd}\right) \tag{15}$$

where, T_e is the torque, and p is the number of pole pairs.

Equation (16) represents both the *Ps* and *Qs* of the machine.

$$\begin{cases} P_s = 1.5(V_{qs} I_{qs} + I_{ds} V_{ds}) \\ Q_s = 1.5(-I_{qs} V_{ds} + V_{qs} I_{ds}) \end{cases} \tag{16}$$

Equation (17) represents the speed expression in terms of torque for the generator.

$$T_e = J\frac{d\Omega}{dt} + f\Omega + T_r \tag{17}$$

STSM technique

STSM approach is a kind of second-order SMC. It is a robust command approach that alters the dynamics of a nonlinear PS by the application of a high-frequency switching command. The basic principle of the STSM approach was suggested by Utkin. It consists of two sections, a continuous section, and a discontinuous section. This approach is detailed in[80,81]. The advantage of the STSM approach is their insensitivity to parameter variations, simple regulator, and no need for the exact model of the machine. This approach has distinctive performance, rapid DR, and high robustness, which qualifies it to be a suitable solution in the field of REs. On the other hand, the STSM approach has been an important technical research field. Today, it is becoming an excellent source of solutions to real-world cons. STSM approach is a kind of variable structure command that possesses strong performances to parameter uncertainties and PS disturbances. The structure of the STSM can be written as follows[82]:

$$\begin{cases} \frac{du_1}{dt} = K_i Sign(S) \\ u = K_p |S|^r Sign\,(S) + u_1 \end{cases} \tag{18}$$

where, *S* is the surface, *Ki* and *Kp* are positive values, *r* is the exponent defined for the STSM.

Figure 3 shows the operating principle of STSM approach.

Due to its high competence, the FMSVM approach was designed to enhance the EE quality and augment the sustainability of the studied PS compared to IVC. In the next subsection, the FMSVM approach, which plays an important role in improving the competence of the RSC of DFIG, is discussed in detail.

Proposed five-level FMSVM approach

The basic principle of the SVM approach was suggested by Der Broek et al. in 1988 and is based on calculating the angle and sector. This approach reduces the THD of voltage and stream and gives 15% more voltage output compared to the PWM. But this technique is more difficult to implement than PWM, especially in the case of multilevel inverters. Using the traditional SVM strategy in the case of a multilevel inverter is very expensive and difficult to achieve experimentally. Therefore, researchers made efforts to improve the characteristics of the traditional SVM strategy and try to create an alternative to it. In[83], a novel SVM technique is based on calculating the minimum (Min) value and maximum (Max) value of 3-phase voltages. This method has been named the modified SVM technique, as it has proven itself well in inverter control. This modulation is simple and easy to

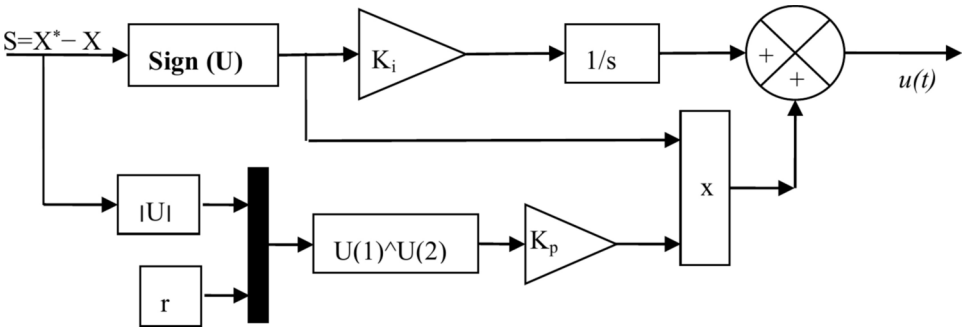

Fig. 3. STSM diagram.

apply compared to the traditional SVM strategy[24]. The modified SVM technique can be applied to control the multilevel inverter with ease, as using this strategy does not require complex calculations as is the case with the traditional SVM strategy. Also, the use of the modified SVM technique in the multilevel inverter allows for reduced implementation costs and ease of experimental implementation. As is known, the control strategy plays an important role in reducing completion costs and improving performance and dynamic response. In[84], the MSVM based on using Max and Min three-phase voltage to control a conventional inverter (two-level) was experimentally verified, and the experiential results were compared with the PWM and traditional SVM strategy. Through the work done in[84], the MSVM approach provided much better results compared to both SVM and NN-SVM techniques, and this is highlighted by the experimental results and simulations performed. The experimental results of the MSVM approach showed its high ability compared to PWM, SVM, and neural SVM techniques in terms of reducing the THD value of current and voltage. These experimental results make the MSVM strategy of interest in this work to be used to control the RSC of DFIG-CRWT.

In this work, the MSVM strategy based on FL approach is used as a suitable solution to control the RSC operation of the DFIG-CRWT system. The RSC is embodied using a five-level reflector in order to obtain excellent results. Using a five-level reflector gives much better results than using a traditional reflector or a four-level reflector. Before discussing the MSVM strategy based on FL approach, you must know the MSVM strategy used to control a five-level inverter. In order to control a five-level inverter using the MSVM strategy, the same principle is used as the MSVM approach used in the work[84]. The Max and Min values of the voltage are calculated first, and then they obtained signals are compared with the triangular signals. To accomplish the MSVM strategy for a five-level reflector, four triangular signals must be used. According to the work done in[84], the MSVM approach for a five-level inverter can be represented in Fig. 4. According to Fig. 4, the MSVM approach for a 5-level inverter is simple, easy to implement, uncomplicated, and inexpensive. By observing the structure of the designer's approach in Fig. 4, it is noted that in this designed technique no voltage components or sectors are calculated. Therefore, it can be said that the five-level MSVM approach is simpler than the classical SVM approach.

In the 5-level MSVM strategy, a HC is used to determine the inverter control pulses. The use of these controls allows the presence of ripples at the current level. Therefore, it is proposed to use the FL approach in this work to replace the use of HC. Therefore, the MSVM approach based on the FL approach is considered a development and

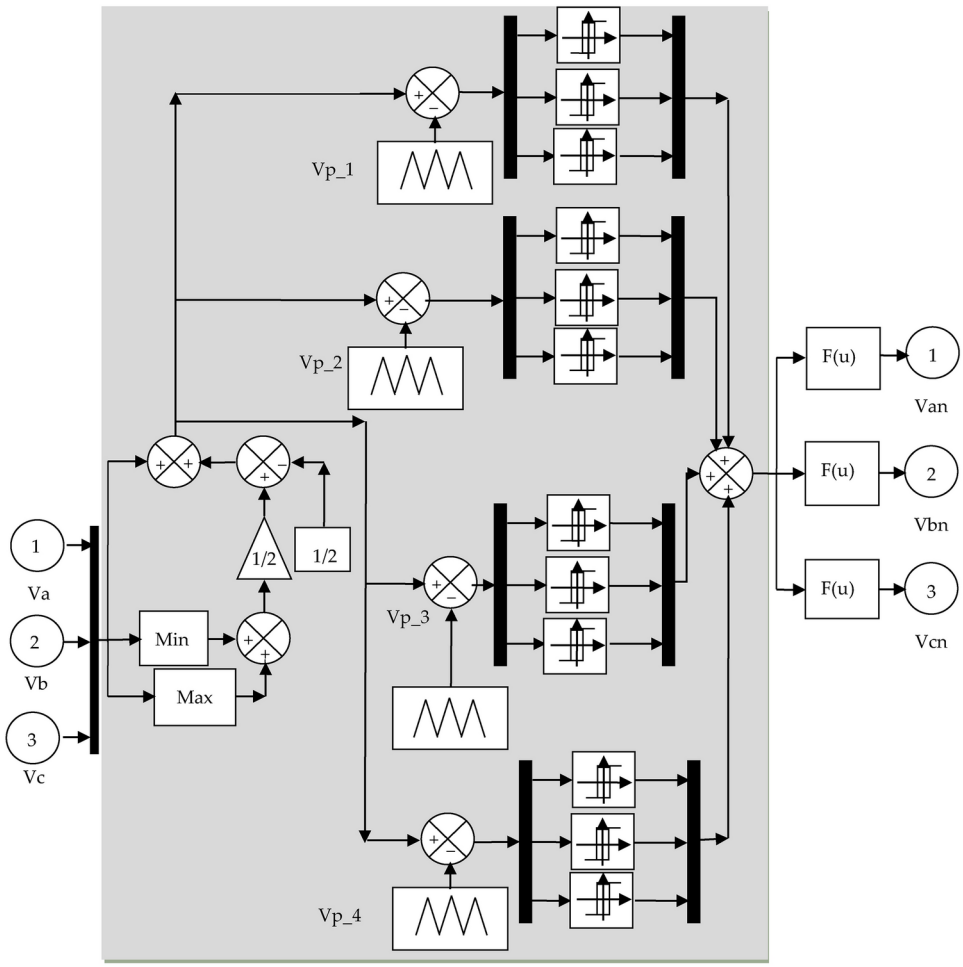

Fig. 4. Structure of 5-level MSVM strategy.

modification of the MSVM approach. The use of FL approach allows to significantly increase the performance and effectiveness of the MSVM approach. A 5-level FMSVM is used to drive the RSC of the DFIG by converting the voltage reference values generated by the IVC-STSMC strategy into pulses.

The structure of the suggested five-level FMSVM approach is given in Fig. 5. This desgined approach is a simple modulation and easy to realize. This designed approach is more robust compared to traditional techniques such as PWM and SVM. The use of this proposed control will also reduce the voltage and current (THD) and improve the characteristics of the studied PS.

The FL approach was relied upon for its many advantages compared to other strategies. Using the FL approach does not require knowledge of the MM of the carefully studied system, which makes it easy to adjust and gives excellent results if the machine parameters change. Also, the use of the FL approach depends largely on experience, as it does not require complex calculations to use and apply it to systems, which makes it one of the best options that can be relied upon. Using the FL approach significantly increases robustness compared to several strategies such as PI control.

In order to obtain better results, the adaptive FL approach was used, where three gains were used in order to better adjust the DR of the FL approach and thus obtain excellent performance for the five-level FMSVM strategy. Figure 6 represents the internal structure of the adaptive FL approach used in this paper, where there are two inputs and only one output.

In this paper, Mamdani type FL approach is used to exemplify the proposed approach. This type was relied upon for its high performance and ease of application. The characteristics of the FL controller used are listed in Table 1.

To embody the five-level FMSVM approach, seven Membership functions (MFs) are used in each entry. Figure 7 represents the MFs used to embody FL approach. MFs are implemented using trigonometric functions. Accordingly, the number of FL rules is 49, which makes the DR of this controller fast and has a distinctive and effective performance. 49 rules were relied upon based on experience and previous work done on FL approach. Table 2 represents the FL rules used to implement the five-level FMSVM technique.

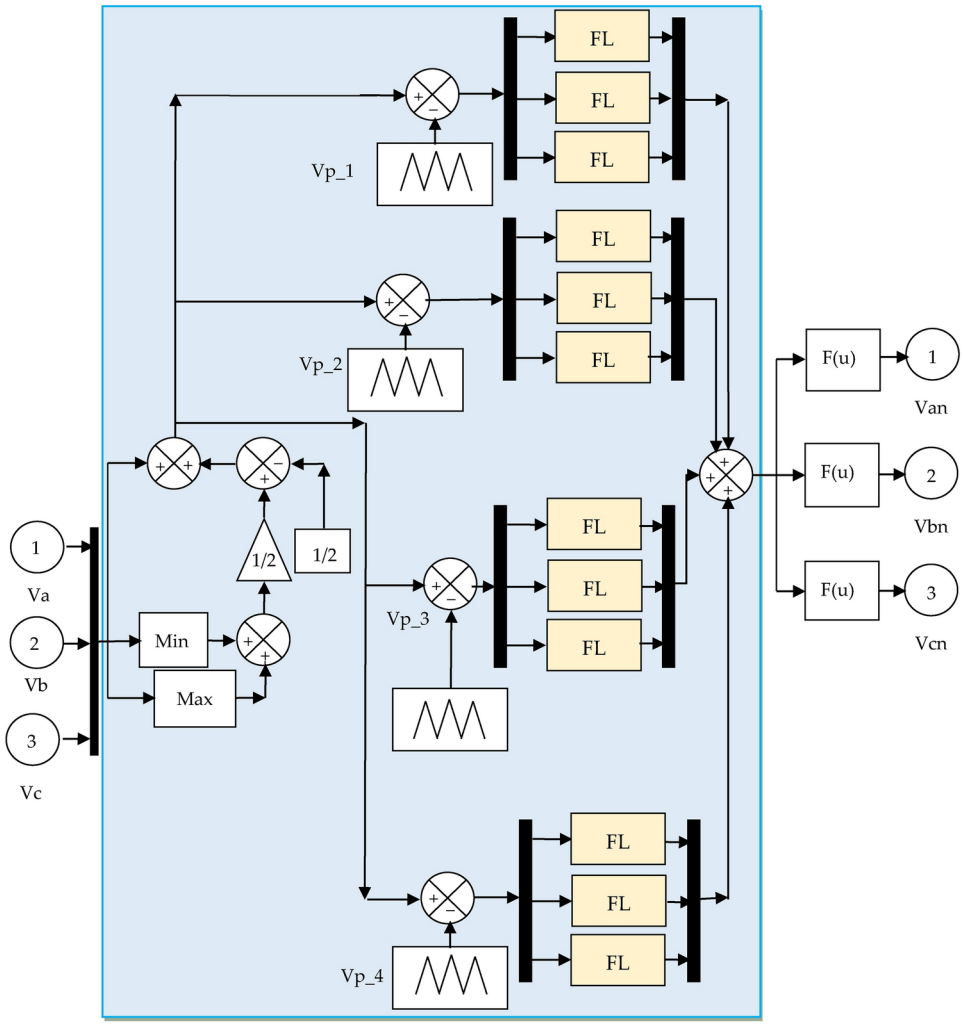

Fig. 5. Structure of five-level FMSVM strategy.

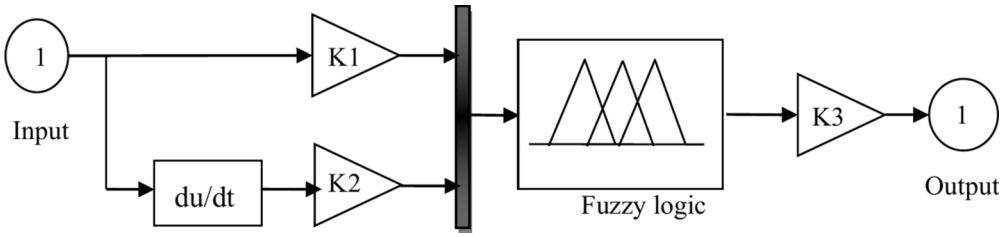

Fig. 6. Construction of the FLC method.

FIS type	Mamdani
Implication	Min
Aggregation	Max
Or method	Max
Defuzzification	Centroid
And method	Min

Table 1. FL approach parameters.

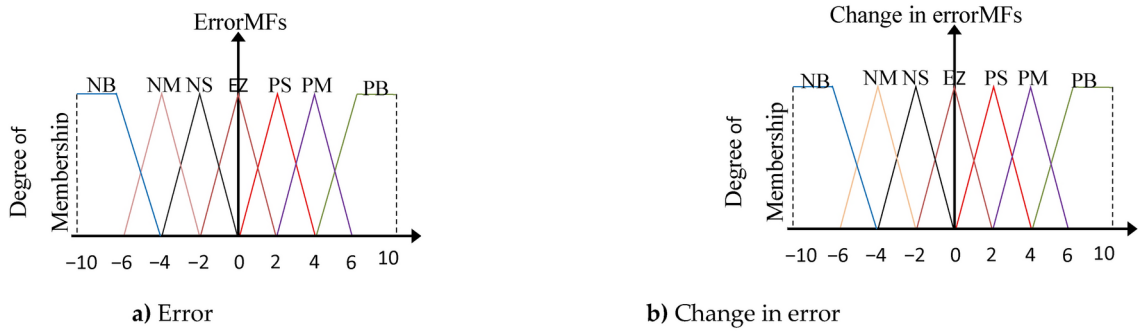

Fig. 7. Membership functions.

e / Δe	NB	NM	NS	EZ	PS	PM	PB
PB	EZ	PS	PM	PB	PB	PB	PB
EZ	NB	NM	NS	EZ	PS	PM	PB
PS	NM	NS	EZ	PS	PM	PB	PB
NB	NB	NB	NB	NB	NM	NS	EZ
PM	NS	EZ	PS	PM	PB	PB	PB
NM	NB	NB	NB	NM	NS	EZ	PS
NS	NB	NB	NM	NS	EZ	PS	PM

Table 2. FL rules of the HCs. Where PM, positive middle; NS, negative small; PB, positive big; NM, negative middle; EZ, equal zero; PS, positive small and NB, negative big.

Proposed robust IVC approach

In this section, a new method is suggested to control the DFIG-CRWT power. To know the MM, the negatives and positives as well as the overall structure, the PI-based IVC approach needs to be addressed first.

Traditional IVC technique

The IVC is considered one of the approaches with rapid DR, as its use in the field of control does not require complex calculations. To use this approach the DFIG MM must be known. The basic idea of the IVC is an indirect technique of the DFIG energy with the PWM. This technique is detailed in[41–43]. The IVC method aims to make the DFIG resemble a direct stream machine, i.e. the change in torque is completely related to the change

in current (the greater the stream, the greater the torque). The IVC approach contains four PI, two for the *Qs* and two for the *Ps*, as well as the PWM approach. To apply the IVC approach to DFIG, Eq. (19) is used for this purpose.

$$\Psi_{qs} = 0 \text{and } \Psi_{ds} = \Psi_s \tag{19}$$

From Eq. (19), the quadrature and direct stator voltages can be written as:

$$\begin{cases} V_{ds} = V_s = w_s \cdot \Psi_s \\ V_{qs} = 0 \end{cases} \tag{20}$$

According to the principle included in Eq. (19), the currents are written according to Eq. (21).

$$\begin{cases} I_{ds} = -\frac{M}{L_s} I_{dr} + \frac{\Psi_s}{L_s} \\ I_{qs} = -\frac{M}{L_s} I_{qr} \end{cases} \tag{21}$$

Equation (22) represents the quadrature and direct of the rotor voltages.

$$\begin{cases} V_{qr} = R_{dr} \cdot I_{qr} + \left(L_r - \frac{M^2}{L_s}\right) w_r \cdot I_{qr} + g\frac{M \cdot V_s}{L_s} \\ V_{dr} = R_{dr} \cdot I_{dr} - w_r (L_r - \frac{M^2}{L_s}) I_{qr} \end{cases} \tag{22}$$

Equations (23) and (24) represent the rotor fluxes and powers, respectively.

$$\begin{cases} \Psi_{dr} = \left(L_r - \frac{M^2}{L_s}\right) I_{dr} + \frac{M}{w_s . L_s} V_s \\ \Psi_{qr} = \left(L_r - \frac{M^2}{L_s}\right) I_{qr} \end{cases} \tag{23}$$

$$\begin{cases} Q_s = -1.5 \left(\frac{\omega_s \Psi_s M}{L_s} I_{dr} - \frac{\omega_s {\Psi_s}^2}{L_s}\right) \\ P_s = -1.5 \frac{\omega_s \Psi_s M}{L_s} I_{qr} \end{cases} \tag{24}$$

The IVC approach aims to determine the reference values for each of the direct and quadrature rotor voltages ($V_{dr}{}^*$ and $V_{qr}{}^*$) based on the error in the DFIG energy. The reference value of V_{dr} is related to the error in the *Qs* and V_{qr} is related to the error in the *Ps*. The error in the energies is calculated between the reference values and the measured values. Therefore, high-precision measuring devices must be used.

The IVC approach is a difficult algorithm in the case of rather complex systems, not robust, and difficult to accomplish compared to the DVC. The IVC is based on using a PI to control the characteristic values (*Qs* and *Ps*). The use of the PI makes the IVC approach affected greatly in case of system parameters change. This control gives more *Ps* and current ripples. This control has a long DR compared to DPC. In terms of the current THD, this control gives a greater value compared to both DPC/DTC.

To enhance the competence and efficacy of this method, a new technique for IVC-PI is proposed in Part 2.4.2. This novel approach is based on the use of both multilevel FMSVM and STSM.

STSM-IVC-FMSVM technique

The disadvantage of the traditional IVC-PI approach is the fluctuations in the flux, torque, and energy. To overcome these drawbacks, an STSM controller and a multilevel FMSVM technique are proposed.

The STSM-IVC technique with a five-level FMSVM (STSM-IVC-FMSVM) is an adjustment of the IVC-PI, where the PI, has been replaced by an STSM. On the other hand, the PWM has been replaced by the proposed multilevel FMSVM technique. Therefore, the STSM-IVC-FMSVM approach is a modification and development of the IVC-PI approach, where four STSM-type controllers were used to control the distinct amounts.

In this work, the gain values of the STSMC controller were adjusted using the experimental and simulation methods. This strategy is fast and gives satisfactory results, as gain values were taken that gave satisfactory results in terms of power quality and THD of current. Using the method of experimentation and simulation to calculate the STSMC controller gain values does not require writing complex programs or large calculations, which makes it the most appropriate method. These gains of the STSMC approach can also be calculated using smart strategies such as using PSO or genetic algorithms (GAs). However, using these strategies requires writing programs, and in some cases, they give unsatisfactory results, which requires repeating the process of calculating the gain values several times.

The STSM-IVC-FMSVM, which is suggested to adjust the DFIG-CRWT power, is shown in Fig. 8, where this approach was applied to the RSC. Controlling this inverter using a highly efficient strategy reduces power ripples and greatly improves current quality. This suggested control is effortless, and easy to apply. This suggested IVC is a more robust control compared to IVC-PI, DTC, DPC, and FOC-PI. This STSM-IVC-FMSVM reduces the *Ps* and *Qs* fluctuations and voltage THD compared to the DVC-PI and IVC-PI.

The STSM-IVC-FMSVM approach relies on a power estimate, and this estimate is used to estimate the energy error. Compared to the IVC-PI, the STSM-IVC-FMSVM approach is described by a significant number of gains, and is experimentally expensive, complex, and difficult to realize. Also, no rule facilitates the use of the FL approach in the MSVM approach to obtain better results, as its use depends on experience and experimentation.

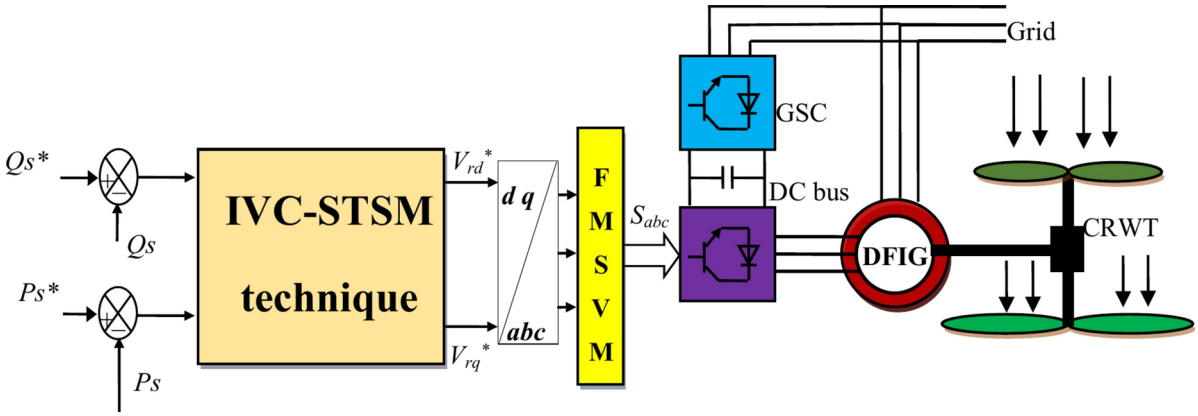

Fig. 8. Proposed IVC of DFIG-CRWT.

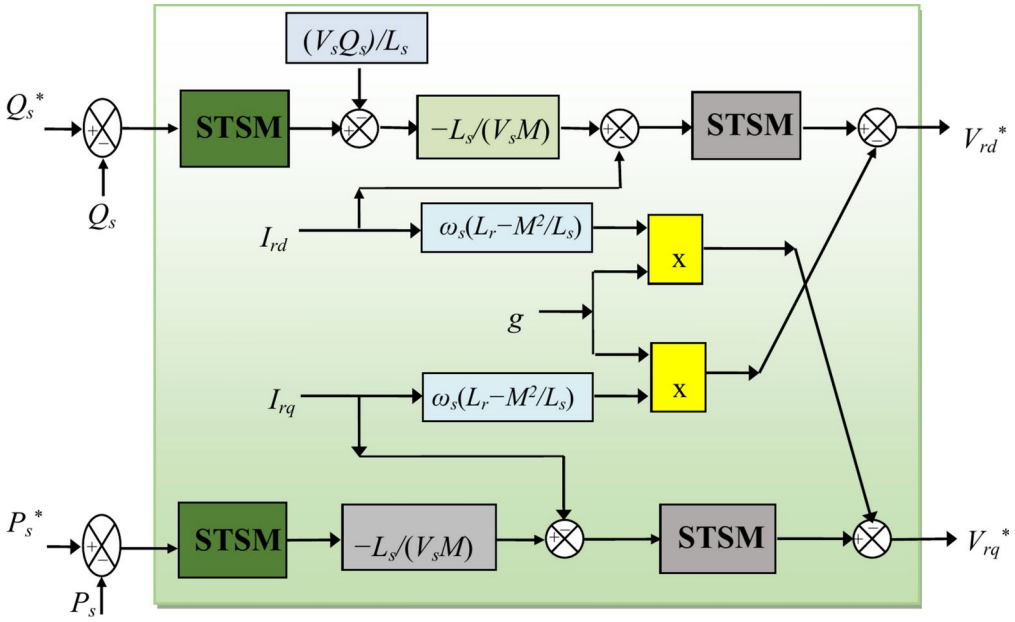

Fig. 9. Internal structure of the designed IVC-STSM approach.

Figure 9 represents the internal structure of the proposed IVC-STSM approach. It is noted that this approach uses an MM of the machine. The use of four STSM controls makes the proposed approach stronger than other controls such as IVC-PI.

To generate the *Vrd** and *Vrq** references, the control scheme in Fig. 9 based on the errors in *Ps* and *Qs* is used. So, the goal of the STSM-IVC-FMSVM approach is to obtain high-precision V_{rd}^{*} and V_{rq}^{*} from the errors in *Ps* and *Qs* for the inverter generator control, errors that tend to zero. To calculate the reference value of *Ps*, the MPPT strategy based on the PI controller is used. This strategy is simple and uncomplicated, so it can be easily accomplished experimentally. Using the PI controller in the MPPT strategy gives a fast DR. Also, using the MPPT strategy makes the *Ps* and current related to the shape of the WS change. Another advantage of using the MPPT strategy is that it protects the WT from strong winds.

A necessary comparative study between the STSM-IVC-FMSVM approach and the IVC-PI, to identify the strengths and weaknesses of both strategies. Table 3 shows a comparative study between the STSM-IVC-FMSVM approach and the IVC-PI approach in terms of regulator used, level of simplicity, ease of application, robustness, etc. Based on this table, it can be said that the STSM-IVC-FMSVM approach is more efficient than the IVC-PI, despite the difficulty of realization. However, the cons of the STSM-IVC-FMSVM approach lie in the simplicity of implementation, as it is less than the IVC-PI. In addition, adjusting the parameters in the STSM-IVC-FMSVM approach is very difficult compared to the IVC-PI, especially in the case of using smart techniques such as GAs, where the time of calculating the parameters is greater in the case of the STSM-IVC-FMSVM approach compared to the IVC-PI, and this is not desirable.

	IVC-PI	STSM-IVC-FMSVM approach
Type controller used	PI	STSM
Modulation	PWM	FMSVM
Level of complexity	Medium	High
Rise time	High	Low
Simplicity of realization	Medium	Complicated
Ease	Medium	Complicated
RT	High	Low
Durability	Low	High
Power ripple	High	Low
THD	High	Low

Table 3. A comparative study between the IVC-PI and the STSM-IVC-FMSVM.

Results

The results (using MATLAB) of the STSM-IVC-FMSVM approach of the DFIG-CRWT are compared with the IVC-PI in terms of the RT, *Ps* and *Qs* fluctuations, THD of stator current, robustness, and tracking references. The proposed command schemes were tested under different tests. The parameters of the DFIG used in this study are the same as those used in[45,48].

Test 1

The first test is represented in the reference tracking test. Simulation results are represented in Figs. 10 and 11. The numerical results of this test are listed in Tables 4 and 5. Figures 10a and b show the current THD for the IVC-PI and STSM-IVC-FMSVM approach, respectively. The given THD value is specific to the network current. It can be observed that the THD is minimized for the STSM-IVC-FMSVM approach (THD = 1.41%) when compared to IVC-PI (THD = 1.72%). Through these results, it can be said that the STSM-IVC-FSVPWM enhanced the THD by about 18.02% compared to the IVC-PI. On the other hand, it is noted that the fundamental signal (FS) amplitude was estimated at 1740 A for the IVC-PI approach and 1738 A for the STSM-IVC-FMSVM approach. Through these values, it is noted that the IVC-PI approach gave a slightly greater length than the STSM-IVC-FMSVM approach. Therefore, it can be said that the amplitude of the FS (50 Hz) is negative according to the STSM-IVC-FMSVM approach in this test. This negativity can be attributed to the gains values of the proposed approach, as this negativity can be overcome in the future by using other strategies such as grey wolf optimization.

The reference and measured *Ps* of the STSM-IVC-FMSVM and IVC-PI are shown in Fig. 10c. From this figure it is noted that the measured value of *Ps* follows well the reference value (Ps_{-ref}). Negative values of the *Ps* indicate that the DFIG is in the state of energy generation, providing power to the grid. In the time domain 0 → 0.5 s and 1.4 s → 1.5 s, the positive values of the *Ps* indicate that the device is in the state of energy consumption (absorption), operating as an electric motor. The STSM-IVC-FMSVM reduced the oscillations of the *Ps* compared to the IVC-PI (Fig. 11a). For the IVC-PI and STSM-IVC-FMSVM, the *Qs* track almost perfectly has its reference value ($Q_{s\text{-}ref}$) (Fig. 10d). Also, the STSM-IVC-FMSVM minimized the *Qs* fluctuations compared to the IVC-PI (Fig. 11b).

The torque is shown in Fig. 10e in the case of both approaches. The amplitudes of the electromagnetic torque depend on the value of the load *Ps* and the state of the drive PS. The STSM-IVC-FMSVM minimized the torque fluctuations compared to the IVC-PI (Fig. 11c).

Figure 10f shows the trajectory of the measured magnitude current of both designed techniques. The value of the current is related to the system and also to the reference value of *Ps* of the DFIG-CRWT system. In addition, the IVC-PI gives more current fluctuations compared to the STSM-IVC-FMSVM approach (Fig. 11d). But, the IVC-PI gives more RT of the torque, *Qs*, and *Ps* compared to the STSM-IVC-FMSVM approach. Figure 10 represents the change in power factor as a function of time for the two approaches. This factor gives a clear picture of the performance of the two approaches, as it is noted that the value of this factor is much better if the designed approach is used compared to the IVC. It is noted that the value of this coefficient is equal to a fixed value and is not affected by changes in WS.

Table 4 represents the value of RT for power and torque. Through this table, it can be said that the STSM-IVC-FMSVM approach improved the RT value compared to the IVC-PI for torque, *Qs* and *Ps* by about 98.60%, 99.05%, and 98.60%, respectively.

The results of this test are abridged in Table 5. Through this table, it can be said that the STSM-IVC-FMSVM approach is better than the IVC-PI in terms of minimizing current and energy fluctuations. Also, in terms of SSE and overshoot of DFIG energy. The STSM-IVC-FMSVM approach minimized the fluctuations of stream, *Qs*, torque, and *Ps* by about 98%, 80%, 93%, and 97%, respectively. These ripple reduction rates are high due to the use of both the STSM controller and multilevel FMSVM in the STSM-IVC-FMSVM approach. In terms of overshoot value of DFIG energy, the STSM-IVC-FMSVM approach provided excellent results compared to the traditional IVC-PI approach. The overshoot values of *Ps* were 1250 W and 350 W for the IVC-PI approach and the STSM-IVC-FMSVM approach, respectively. Therefore, the STSM-IVC-FMSVM approach minimized the overshoot of *Ps* by an estimated ratio of 72%. The overshoots of *Qs* were 2700 KVA and 450 KVA for the IVC-PI approach and the STSM-IVC-FMSVM approach, respectively. Therefore, the STSM-IVC-FMSVM approach

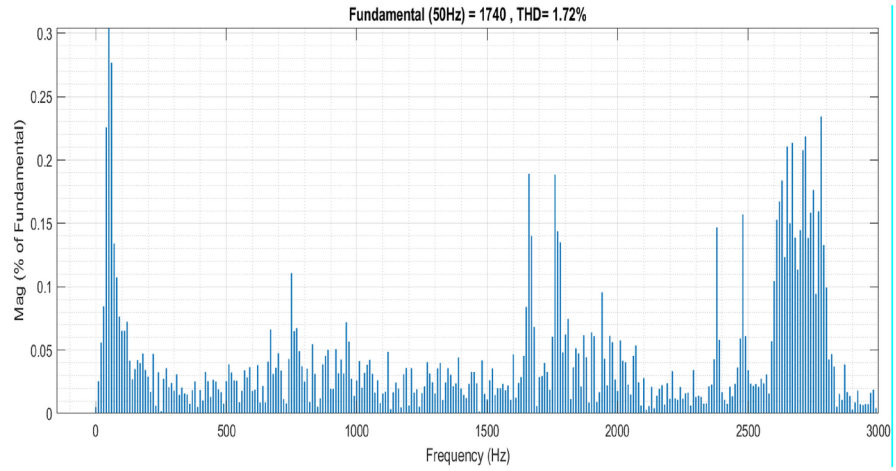

a)THD (IVC-PI).

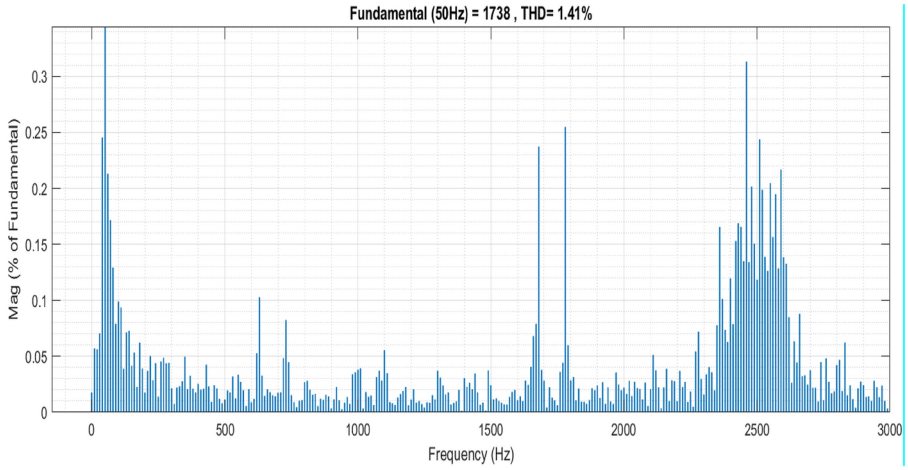

b)THD (STSM-IVC-FMSVM**)**

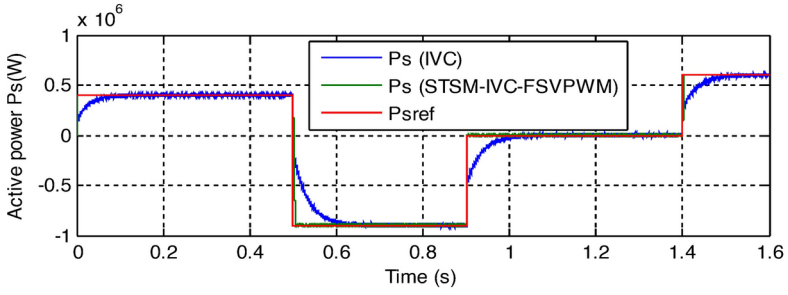

c)*Ps*.

Fig. 10. Test 1 results.

significantly reduced the overshoot value of *Qs*, which indicates great performance of the proposed approach, as this reduction was estimated at 83%.

From Table 5 it is noted that the SSE value of DFIG energy was low when using the STSM-IVC-FMSVM approach compared to the IVC-PI approach. The SSE value of *Qs* was 2150 VAR and 320VAR for both the IVC-PI technique and the STSM-IVC-FMSVM approach, respectively. These values indicate that the STSM-IVC-FMSVM approach significantly minimized the SSE of *Qs* by an estimated ratio of 85%. Also, the STSM-IVC-FMSVM approach significantly reduced the SSE of *Ps*, as its value was estimated at 1150 W and 280 W for the conventional IVC and STSM-IVC-FMSVM, respectively. Therefore, the ratio of minimization in SSE of *Ps* was estimated at 76%. Also, the use of FL in systems greatly helps to enhance efficiency and overcome defects.

The ratios mentioned above for the THD and ripples' reduction have been estimated by the reduction ratio (RR) of the THD (RR_{THD}), the current ripple ($RR_{current}$), the torque ripple (RR_{torque}), *Ps* ripple (RR_P) and *Qs* ripple (RR_Q) given by Eqs. (25–29):

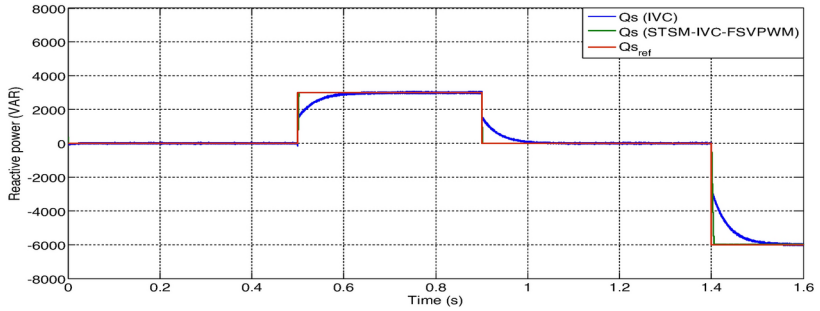

d)*Qs*.

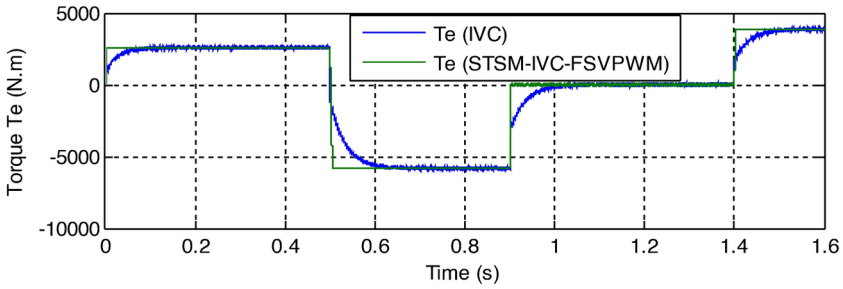

e) Torque.

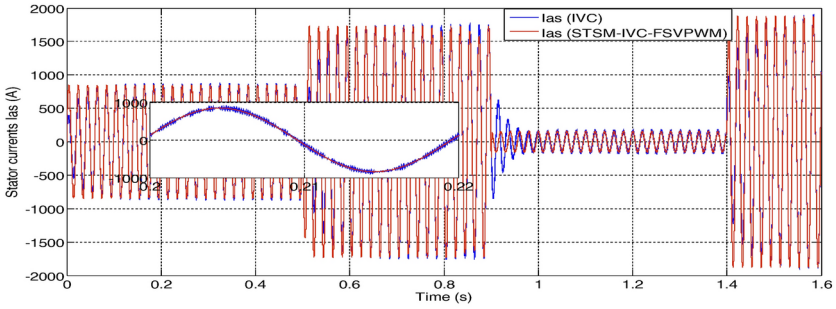

f)Current.

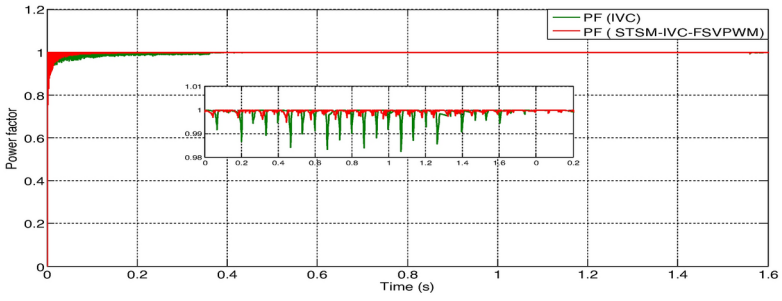

g)Power factor

Figure 10. (continued)

$$RR_{THD}(\%) = \frac{THD_{S1} - THD_{S2}}{THD_{S1}} \tag{25}$$

$$RR_{current}(\%) = \frac{I_{S1} - I_{S2}}{I_{S1}} \tag{26}$$

$$RR_{torque}(\%) = \frac{T_{S1} - T_{S2}}{T_{S1}} \tag{27}$$

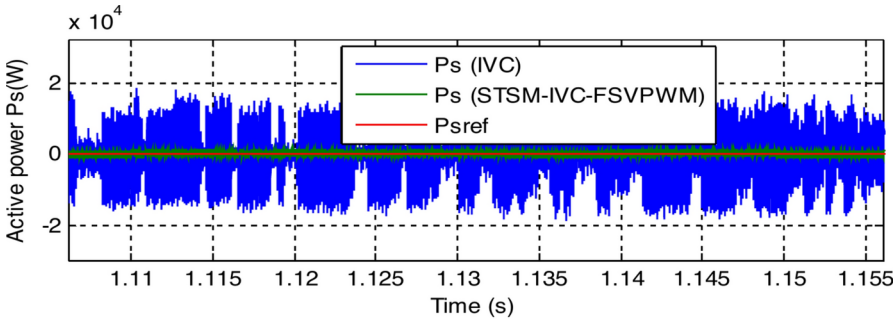

a)*Ps*.

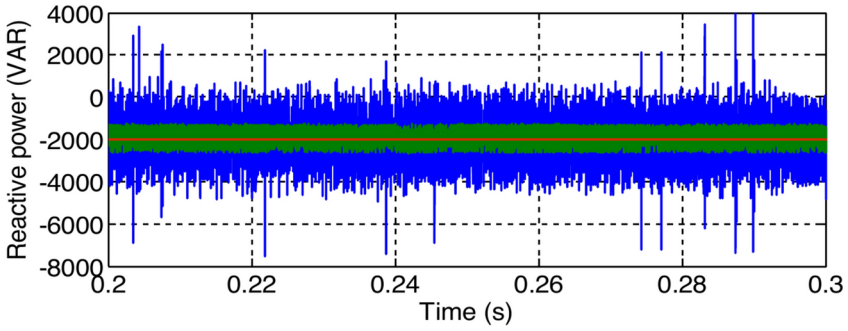

b)*Qs*.

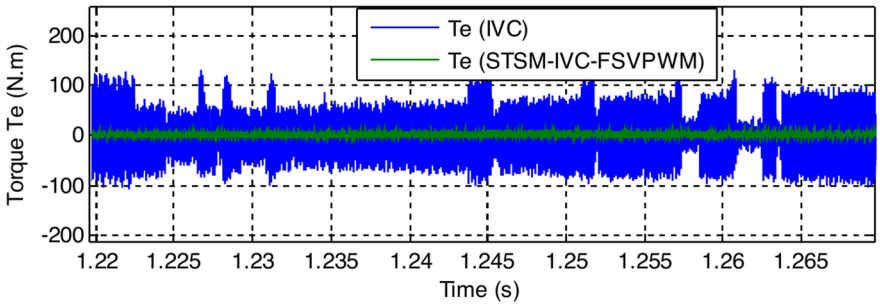

c)Torque.

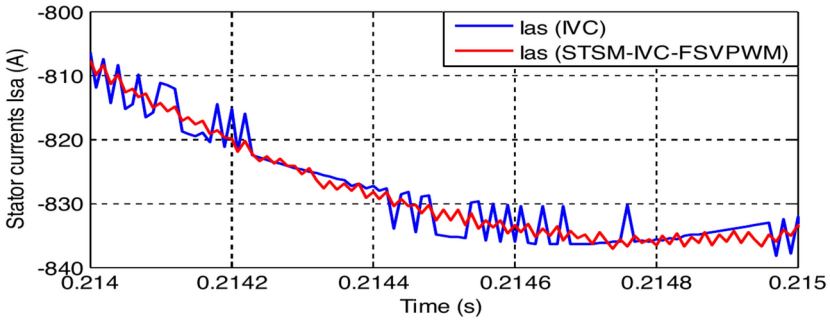

d)Stream

Fig. 11. Zoom in the results of test 1.

	RT		
	Torque	*Qs*	*Ps*
IVC-PI	0.098 s	0.09 s	0.098 s
STSM-IVC-FMSVM	1.374 ms	0.85 ms	1.37 ms
Ratios	98.60%	99.05%	98.60%

Table 4. RT of power and torque.

Criteria		Strategies	
		Traditional IVC strategy	STSM-IVC-FMSVM approach
Time response (s)		High	Low
THD (%)		1.72	1.42
Reference energy tracking		Satisfactory	Excellent
Energy fluctuations		High	Very weak
Overshoot	*Qs* (VAR)	2700	450
	Ps (W)	1250	350
Qs fluctuations (VAR)		4500	900
Torque fluctuations (N.m)		210	15
Settling time (ms)		High	Low
Durability		Low	High
Rise time (s)		High	Low
Ps fluctuations (W)		36,000	1100
Converter and filter design		Simple	Simple
Current ripple (VAR)		60	1
SSE	*Qs* (VAR)	2150	320
	Ps (W)	1150	280
Algorithm difficulty		Simple	Complicated
Lively performance		Low	High
Fineness of the energy generated		Low	High

Table 5. Comparative results obtained from the STSM-IVC-FMSVM with the IVC-PI.

$$RR_P(\%) = \frac{P_{S1} - P_{S2}}{P_{S1}} \tag{28}$$

$$RR_Q(\%) = \frac{Q_{S1} - Q_{S2}}{Q_{S1}} \tag{29}$$

where THD_{S1}, I_{S1}, T_{S1}, P_{S1} and Q_{S1} represent the THD value and fluctuations value for the torque, stream, and *Ps* and *Qs* of the IVC-PI (S1), and THD_{S2}, I_{S2}, T_{S2}, P_{S2} and Q_{S2} represents the values for the same variables of the STSM-IVC-FMSVM(S2).

In order to confirm these results, in the following test, the parameters of the DFIG are changed, through it, the effect of the STSM-IVC-FMSVM approach was studied compared to the IVC-PI method.

Test 2

This test is different from the previous test. In this test, the robustness of the proposed approach is studied compared to the traditional IVC approach in terms of changing DFIG parameters. In Test 2, the nominal values of L_s and L_r are multiplied by 0.5, and R_s and R_r are multiplied by 2. Figures 12 and 13 represent the results obtained. The numerical results of this test are listed in Tables 6 and 7.

Figures 12a and b represent the THD of current for two controllers. The value of THD was 1.85% for the traditional IVC approach and was estimated at 1.55% for the proposed approach. So, the proposed approach reduced the THD value compared to the traditional IVC technique by an estimated percentage of 16.22%, as shown in Table 6. However, in terms of FS amplitude (50 Hz), the proposed approach gave amplitude slightly less than the conventional IVC approach. The amplitude value was 1740 A and 1739 A for both the conventional IVC approach and the proposed approach, respectively. It can be concluded that the FS amplitude (50 Hz) is the negative of the proposed approach in this test. This negative can be overcome in the future by using smart strategies to calculate the gains of the proposed approach.

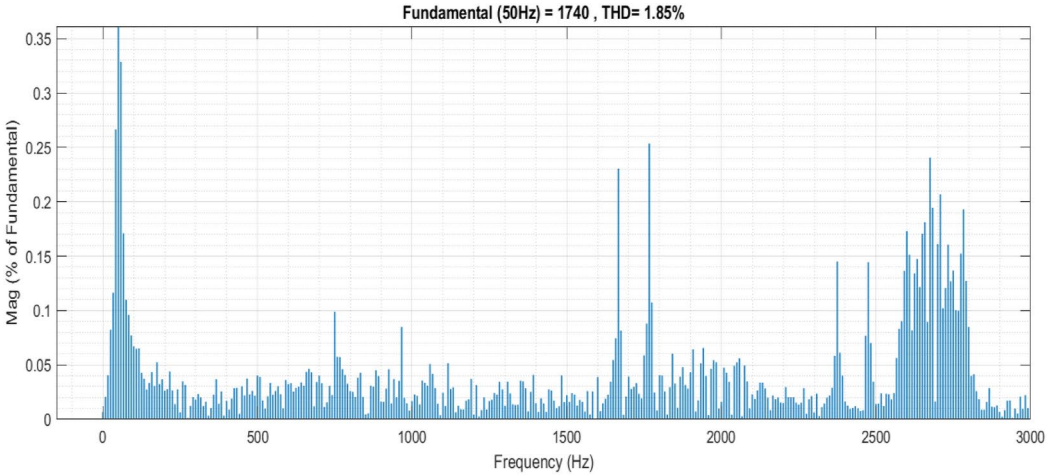

a)THD (IVC-PI).

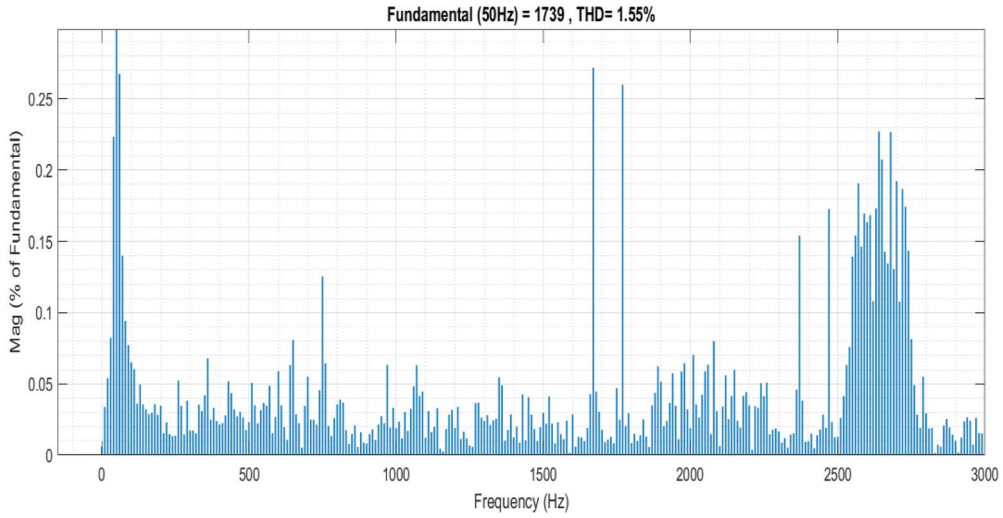

b)THD (STSM-IVC-FMSVM).

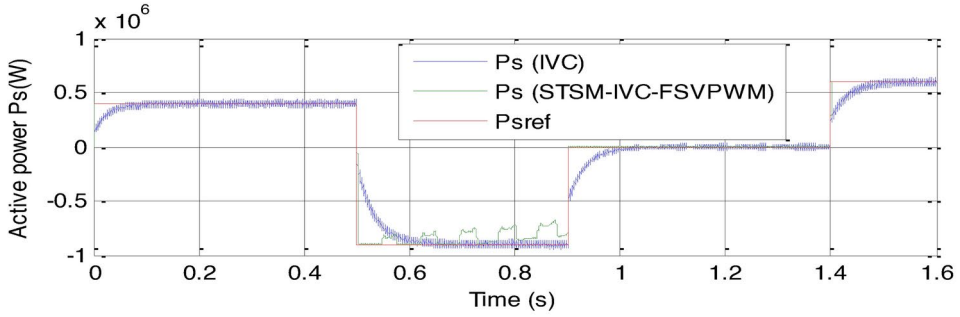

c)*Ps*.

Fig. 12. Test 2 results.

Changing the DFIG parameters has a clear effect on torque, current, and power. This effect is huge if the IVC-PI is used compared to the STSM-IVC-FSVPWM approach (Fig. 12c–f). This effect appears clearly in the fluctuations of power, stream, and torque of the two approaches (Fig. 13a–d). Also, it is noted that despite the change in the DFIG parameters, the measured values of the energies (*Qs* and *Ps*) still follow the reference values well with a fast DR of the two controls. The *Ps* keeps taking negative values and its change is the same as the change in WS. However, it is noted that the STSM-IVC-FMSVM approach provided an unsatisfactory RT compared to IVC-PI in case of changing device parameters. Therefore, RT is the only negativity of the control

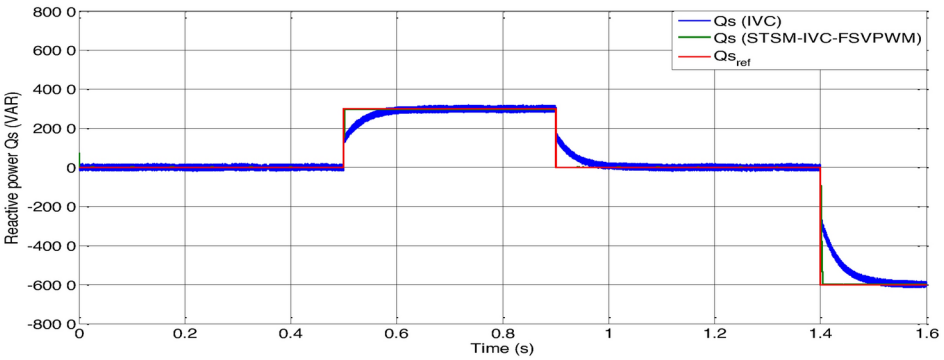

d) Qs.

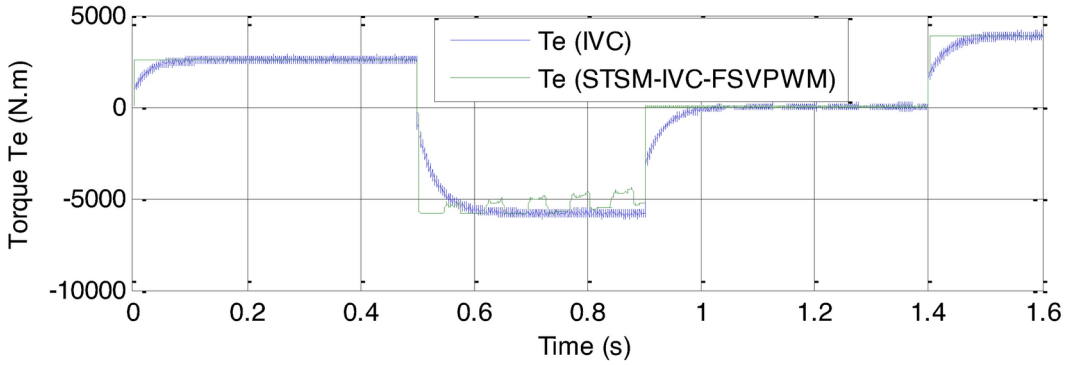

e) Torque.

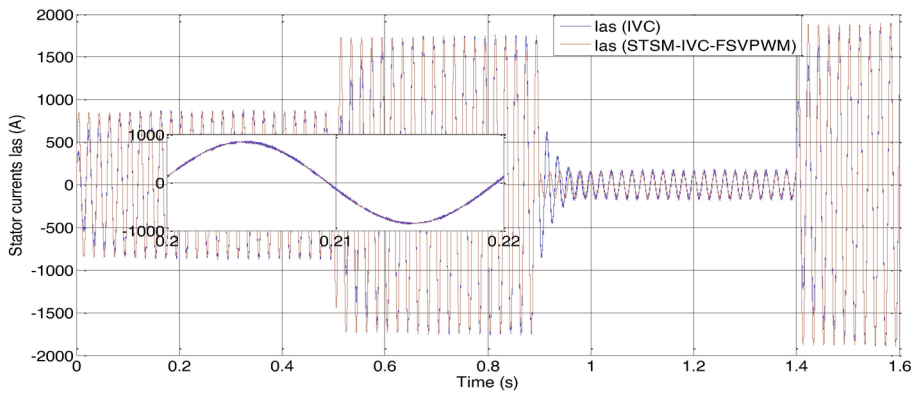

f)Stream.

Figure 12. (continued)

designed in this test. This negativity is attributed to the gain values of the STSM-IVC-FMSVM approach, values that were estimated by trial and error through simulation, but which in future work can be optimally estimated using intelligent algorithms.

In this test, it is observed that the torque and stream keep changing according to the change in the *Ps* (Fig. 12e and f), which are the same observations as in the first test. Also, torque has negative values, as is the case with *Ps*, which indicates that the machine is generating EE. The current remains sinusoidal for the two approaches, with the STSM-IVC-FMSVM approach having an advantage in terms of current fineness, as shown in Fig. 13d. Figure 12g represents the power factor as a function of time for the two approaches. This parameter takes a fixed value equal to 1 for both controls despite the change in parameters, as it is observed that there are fluctuations at the level of this parameter. The power factor fluctuations are less when using the proposed approach compared to the IVC-PI approach. Table 7 represents the numerical values for each of the ripples, overshoot, and SSE of DFIG power. In Table 7, the ripple values of current, energy, and torque for the two control elements are listed, where the reduction ratios that highlight the superiority of the STSM-IVC-FMSVM approach are calculated.

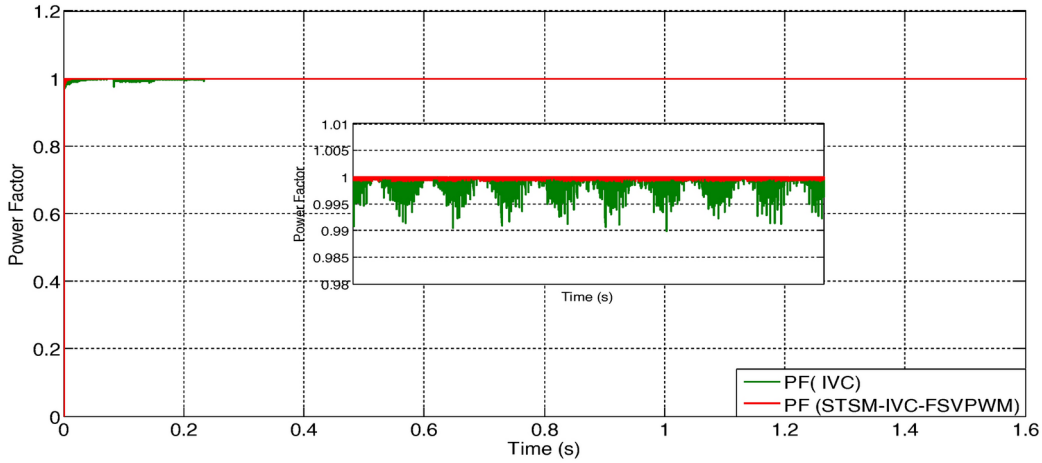

g)Power factor

Figure 12. (continued)

From this table, it appears that STSM-IVC-FMSVM compared to IVC-PI minimized current, *Qs*, torque and *Ps* ripples by about 95%, 93%, 95.23%, and 97% respectively. The STSM-IVC-FMSVM approach provided excellent results in terms of SSE and overshoot of the DFIG power compared to the IVC approach. In the case of SSE of *Ps*, the STSM-IVC-FMSVM approach reduced this value by an estimated 72% compared to the IVC approach. Also, the STSM-IVC-FMSVM approach reduced the SSE value of *Qs* by an estimated 92% compared to the IVC. The STSM-IVC-FMSVM approach minimized the overshoot of *Ps* and *Qs* by 72% and 92%, respectively, compared to the IVC approach. These high percentages indicate high performance and the strength of the designed approach in improving the features of the studied PS. The rate mentioned above for the THD, overshoot, SEE, and ripples' reduction has been estimated by using the same Eqs. (25–29), but with the values mentioned in Table 7.

In this test, it is noted that there are two negative aspects of the STSM-IVC-FMSVM as a result of changing the system parameters, and this is because the STSM-IVC-FMSVM is related to the DFIG-CRWT parameters (*Rs*, *Ls*, *Rr*, and *Lr*). These two negatives are represented in the presence of fluctuations in the case of *Ps* that are large (in the time domain from 0.5 to 0.8 s), and the second negative is represented in the double amplitude (lower amplitude compared to the first test) of the FS compared to the IVC-PI, as this value was 1739 A compared to 1740 A for the IVC-PI. This problem of STSM-IVC-FMSVM can be fixed in the future by using smart techniques to identify the optimal values for gains.

Discussion

The fluctuations of the current (*I*), torque (*T*), *Ps* (*P*) and *Qs* (*Q*) have been estimated for both analysed approaches (S_i, where i = 1 and 2 means the classical IVC approach and the proposed STSM-IVC-FMSVM approach) under two tests. In the test 2 the nominal values used in the test1 for the R_s and R_r are multiplied by 2 and L_s and L_r are multiplied by 0.5.The values of the robustness indicator regarding the percentage increase of the fluctuations of the *I*, *T*, *P*, and *Q* are registered in Table 8.

In Table 9, the influence of the stream THD and the value of the amplitude of the FS (50 Hz) of stream signal between the two control tests are studied, where the influence ratios for the two values are calculated. This table gives a clear picture of the use of the two types of control on the values of both amplitude and THD. From Table 9, it is noted that the FS amplitude value (50 Hz) was not significantly affected in the second test compared to the first test. The difference in amplitude between the two tests was estimated as 0 A and 1 A for both the traditional IVC-PI approach and the proposed approach, respectively. Therefore, the STSMC-IVC-FMSVM approach gave the largest difference in amplitude value compared to the IVC-PI approach.

The THD value for the two controls increased significantly in the second test compared to the first test as a result of changing the DFIG parameters. The difference in the THD value between the two tests was estimated to be + 0.13% and + 0.14% for IVC-PI and STSMC-IVC-FMSVM, respectively. Accordingly, the STSMC-IVC-FMSVM approach presented the largest difference compared to the IVC strategy and negative margins. This difference was estimated to be 7.03% and 9.03% for IVC-PI and STSMC-IVC-FMSVM, respectively. Although the STSMC-IVC-FMSVM approach provided good THD values in both tests, the percentage change of THD value was greater when using the STSMC-IVC-FMSVM approach compared to the conventional approach, which can be attributed to the gain values of the STSMC-IVC-FMSVM approach. The drawbacks of the proposed approach can be overcome in the future by using intelligent methods to calculate the gain values for this approach.

The values mentioned in Table 8 highlight the better robustness of the STSM-IVC-FMSVM compared to the IVC-PI.

Finally, a comparative study between the STSM-IVC-FMSVM and several available articles in terms of THD[54,85–87]. The results were collected in Table 10. By noting this table, we find that this STSMC-IVC-FSVPWM in this work gave a THD value much less than several approaches that have been published in other scientific

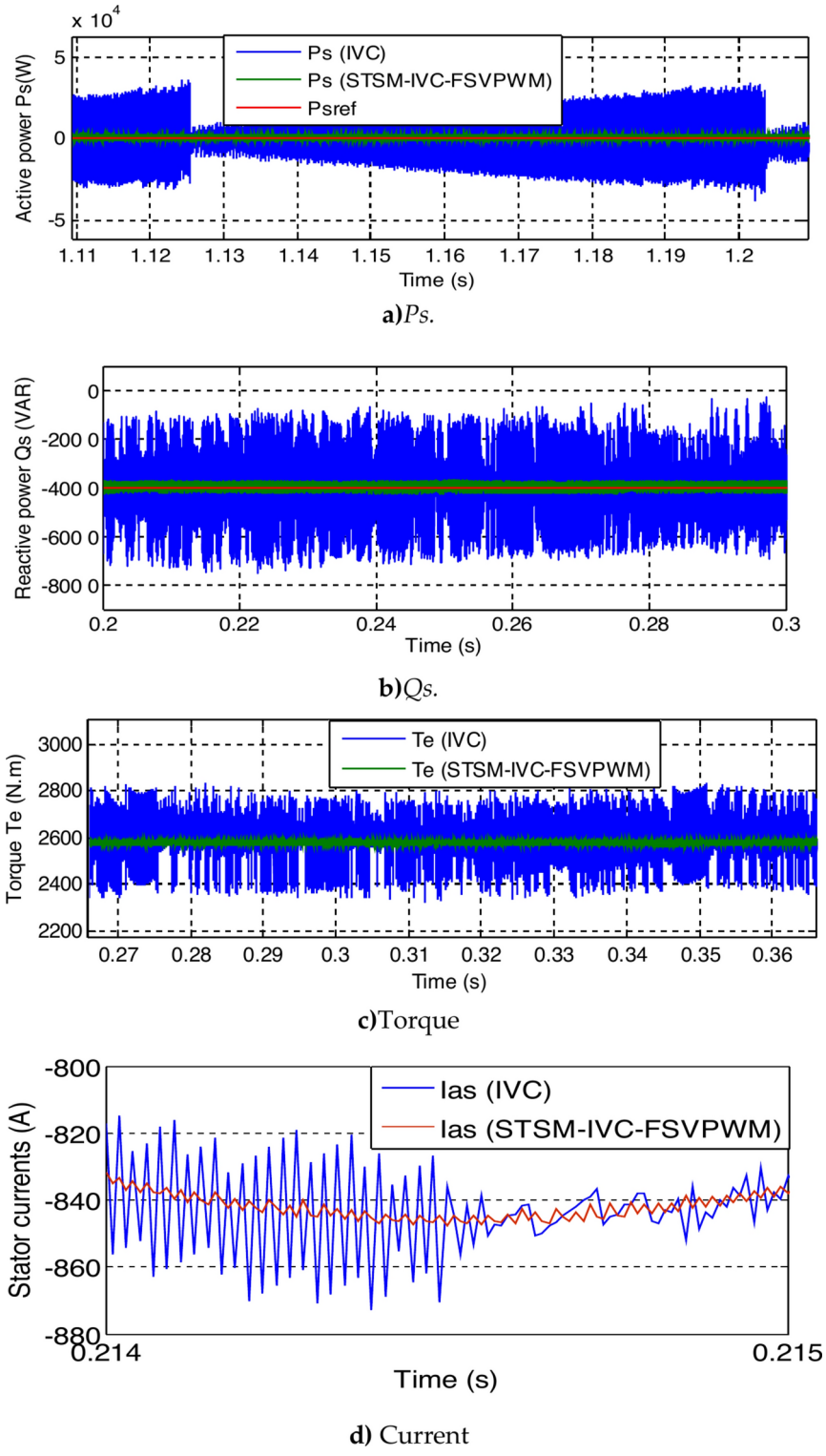

Fig. 13. Zoom in the results of test 2 (power, current, and torque).

works, including experimental work. This indicates that this approach is performant. Moreover, it can be easily accomplished compared to BC approach or passivity control.

The TR obtained in this paper can be compared with different approaches studied in[54,87–90]. We find that this proposed IVC provided a very small time compared to NN-second order SMC and DPC. Through the results of the blog in the Table 11, it can be said that the STSM-IVC-FMSVM improved the value of the RT compared to the DPC for each of the torque, *Qs* and *Ps* by about 92.36%, 95%, and 92.36%, respectively. And by about 72.52%, 90.55%, and 72.52%, respectively, compared with the NSOSMC approach.

	Current (*Ias*)		
	IVC	STSM-IVC-FMSVM	Ratios (%)
THD (%)	1.85	1.55	16.22
FS amplitude (50 Hz)	1740 A	1739 A	−0.06

Table 6. THD and of the both techniques.

		IVC-PI	STSM-IVC-FMSVM	Ratios (%)
Torque fluctuations (N.m)		420	20	95.23
Fluctuations	*Qs* (VAR)	6500	425	93
	Ps (W)	37,500	1250	97
Current fluctuations (A)		100	5	95
SSE	*Qs* (VAR)	1950	190	92
	Ps (W)	1240	350	72
Overshoot	*Qs* (VAR)	2350	190	92
	Ps (W)	1450	410	72

Table 7. Comparative fluctuations obtained from the IVC-PI with the STSM-IVC-FSVPWM.

Robustness indicator	Designed control techniques	
	IVC (%)	STSMC-IVC-FMSVM (%)
$(I_{Si(test2)} - I_{Si(test2)})/I_{Si(test1)}$[%]	40	4
$(T_{Si(test2)} - T_{Si(test2)})/T_{Si(test1)}$[%]	210	5
$(P_{Si(test2)} - P_{Si(test2)})/P_{Si(test1)}$[%]	14,000	100
$(Q_{Si(test2)} - Q_{Si(test2)})/Q_{Si(test1)}$[%]	45,000	200

Table 8. Robustness indicators.

		IVC-PI	STSMC-IVC-FMSVM
Amplitude of FS (50 Hz)	Test 1	1740 A	1738 A
	Test 2	1740 A	1739 A
	Test 2 – Test 1	0 A	+1
	Ratios (%)	0	0.06
THD (%)	Test 1	1.72	1.41
	Test 2	1.85	1.55
	Test 2 – Test 1	+0.13	+0.14
	Ratios (%)	7.03	9.03

Table 9. Study of the change in values of FS (50 Hz) amplitude and stream THD between the second and first tests.

Tables 12 and 13 represent a comparison with other related works in terms of fluctuations minimization ratios, undershoot, and SSE of DFIG energy. By observing Table 12, the designed approach provided much better reduction rates for both overshoot and SSE than several approaches. This table highlights the significant superiority of the designed approach and its ability to enhance the values of both overshoot and SSE. In Table 13, it is noted that the designed approach provided much better ratios for reducing the ripples of both *Ps* and *Qs* than other strategies. This table shows that the proposed approach gave high energy quality compared to other approaches, which makes it a reliable solution.

The results obtained above are proven using experimental work, where HIL testing was used to prove this performance of the proposed approach. The dSPACE 1104 was used to complete this experimental work, and all the details and experimental results are in the next section.

Experimental results

To verify the effectiveness/feasibility of STSMC-IVC-FMSVM in real time, the HIL test is used. HIL testing is a method by which the effectiveness and safety of strategies are experimentally verified within a short time without

References	Commands	THD (%)
[85]	DTC	6.70
	Fuzzy DTC	2.40
[86]	Multi-resonant-based SMC	3.14
	Integral SMC	9.71
[27]	DFOC-PI	1.45
[41]	Field-oriented control	3.7
[45]	VC	2.20
	Adaptive BC-SMC	1.15
[48]	DPC-SMC	1.66
[54]	SMC	2.56
Designed approach	Test 1	1.41
	Test 2	1.55

Table 10. Comparative results with other controls.

		RT (ms)		
		Torque	*Qs*	*Ps*
TSM-IVC-FMSVM		1.374	0.85	1.37
Ref. [54]	DPC	18	17	18
	NN-second-order SMC (NSOSMC)	5	9	5
Ref. [87]		–	80	15
Ref. [88]		–	34.50	33.80
Ref. [89]		12.15	10.08	12.15
		11.25	9.85	11.25
		11.85	10.05	11.85
Ref. [90]		0.9	2.10	0.9
		2.50	3	2.50
		2.65	3.25	2.65
		4.80	5.40	4.80

Table 11. RT analysis.

the need for extensive equipment or high costs. The advantage of using the HIL test is that it does not require complex technology or large programs, which makes it the most suitable experimental method.

In this part, the HIL test was relied upon to experimentally verify the validity of the proposed approach (STSM-IVC-FMSVM) and compare it with the traditional approach (IVC-PI). Figure 14 represents the completed HIL test of the proposed approach and the necessary equipment needed to complete this experimental work. HIL testing was used using the dSPACEDS1104R&D control board (developed by the German company dSPACE to optimize high-speed multivariable digital regulators and real-time simulations). This board can be plugged into a PCI slot of a PC (see Fig. 14b). It consists of two processors: a master processor to manage the application, and a slave processor, a Digital Signal Processor based on the MPC 8240 microcontroller, which generates the PWM signals. This board is connected to MATLAB and Simulink through a tool called RTI (Real-Time Interface). This tool allows access to the inputs/outputs of the board while developing the model in Simulink. Additionally, it facilitates the implementation of the Simulink model into the board by converting it into C programming code. This code is subsequently transferred to the DS1104 board using software that is independent of MATLAB/Simulink called Control Desk (CD). The latter not only loads the code onto the board but also facilitates real-time monitoring and system control. Therefore, the implementation of the STSMC-IVC-FMSVM in the dSPACE DS1104 hardware can be summarized in four essential steps:

Step 1 Create and design the control PS model in MATLAB.

Step 2 Generate code C from the Simulink control model using the RTI.

Step 3 Download the generated code into the DS1104 board using the CD software.

Step 4 Execute the control system in real-time and visualize the results using the CD software.

Figure 14 illustrates the communication between the DFIG-CRWT system and the dSPACE DS1104 board. In the HIL test, the actual shape of the generator or turbine is not used. Therefore, first, the validity of the studied PS is verified using MATLAB and then verified using the HIL test. Accordingly, the DFIG generator is given an MM and is implemented in the MATLAB program. As shown in Fig. 14b, using the HIL test requires using a media device that includes MATLAB 2021.

In Fig. 15, the experimental results obtained from this study for the control approaches are shown. The WS used is represented in Fig. 15a. The *Ps* is represented in Fig. 15b, where it is noted that the *Ps* of the two

		SSE ratios		Overshoot ratios	
		Ps	*Qs*	*Ps*	*Qs*
Ref [91]		–	–	7.23%	16.59%
		–	–	74.46%	48.53%
		–	–	31%	21.74%
Ref [92]		35%	36.93%	–	–
Ref [93]	Test 1	28.76%	76.55%	25.07%	6.44%
	Test 2	30.48%	24.62%	9.19%	6.05%
Ref [94]		45.83%	78.44%	–	–
		56.52%	52.22%	–	–
		87.50%	48.75%	–	–
Ref [95]		–	–	73.83%	48.38%
		–	–	77.58%	82.76%
		–	–	20.10%	49.32%
Ref [96]		50%	38.32%	32.20%	44.06%
		40%	39.68%	32.49%	22.77%
Ref [97]		–	–	51.49%	62.55%
		–	–	62.85%	70.83%
		–	–	59.79%	67.34%
Designed technique		76%	85%	72%	83
		72%	92%	72%	92%

Table 12. Comparison in terms of SSE and overshoot.

Approaches		Ratios	
		Qs ripples (%)	*Ps* ripples (%)
Proposed approach		80	97
		93	97
Ref [94]		56.66	54.25
		46.68	47.50
		50.75	50.41
Ref [97]	DPC with NN algorithm	45.26	66.29
	Neuro-fuzzy-DPC	57.74	67.13
Ref [92]		36.93	22.95
		78.12	86
		78.42	80.18
Ref [95]		50	44.50
		52.98	63.33
		48.18	50
Ref [98]. (Modified SC technique)		45.26	92.85
		73.33	84.50
		43.07	33

Table 13. Comparison in terms of fluctuations of the DFIG power.

controllers follows the reference well, with larger fluctuations in the case of IVC-PI-PWM compared to STSM-IVC-FMSVM. Also, it is noted that the RT of the *Ps* when using STSM-IVC-FMSVM is much better than the RT using IVC-PI-PWM and these are close to the simulation results. In Fig. 15c, the *Qs* response of the two controls is shown. From this figure it is observed that the *Qs* of the two controllers follow the reference well, with STSM-IVC-FMSVM having an improvement in terms of RT and fluctuations compared to IVC-PI-PWM. These results show the superiority of STSM-IVC-FMSVM over IVC-PI-PWM, as these results confirm what was obtained in the simulation section, which is a positive thing. The torque of the DFIG in the case of two controls is represented in Fig. 15d, where it is noted that the torque has the same form as the *Ps*. It takes positive values in the case of the *Ps* having a positive value and is negative when the *Ps* is negative. Also, it is noted that STSM-IVC-FMSVM provided much better fluctuations and torque RT than IVC-PI-PWM, which are the same simulation results. In Fig. 15e and f, the changes in both stator and rotor current for the two controls are shown. These two currents change according to the change in *Ps*, as their value decreases and increases with the decrease and

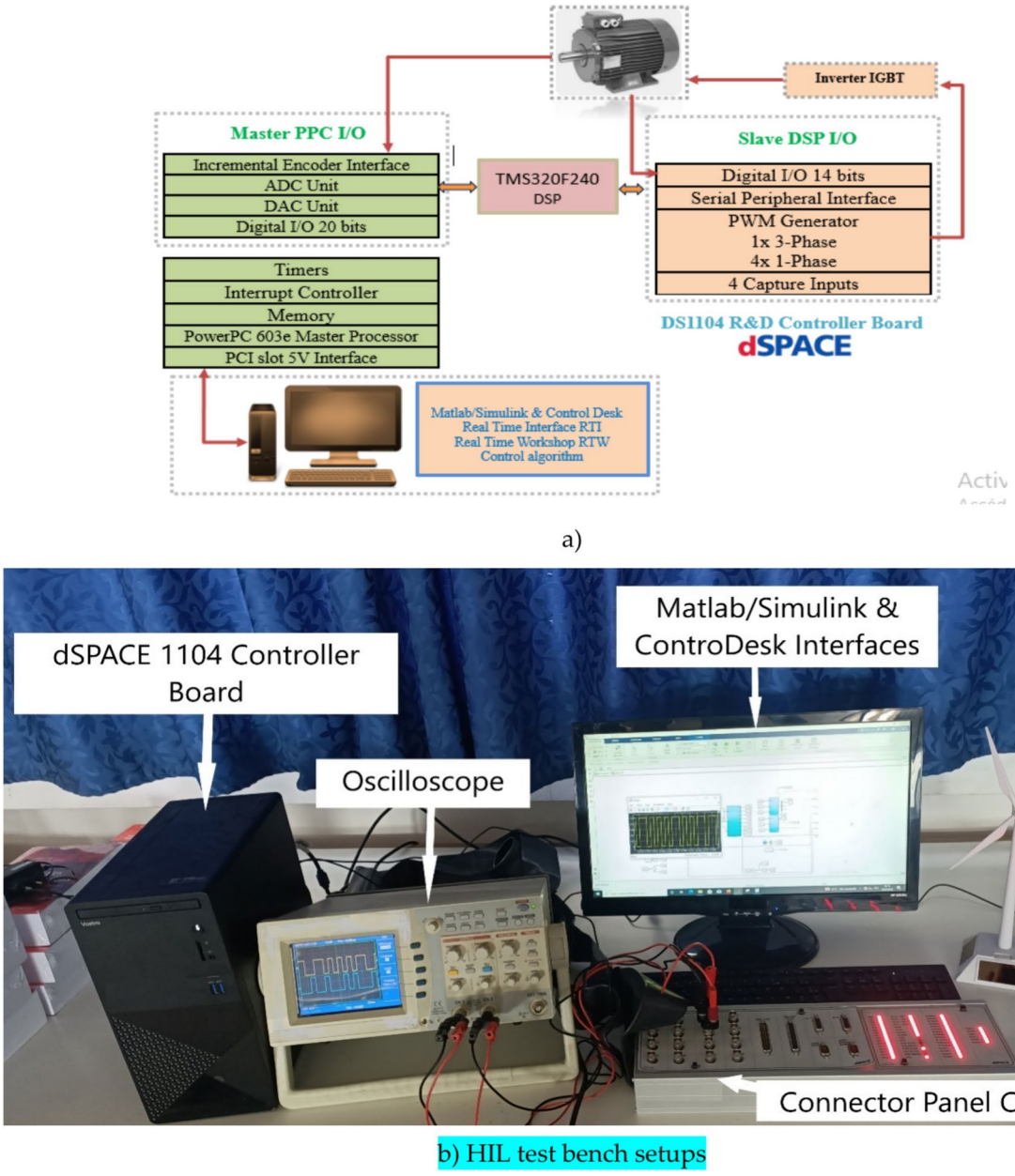

Fig. 14. Schematic diagram of HIL simulation system.

enhance in the value of *Ps*. Also, it is noted that the shape of the stream is sinusoidal for both approaches, with STSM-IVC-FMSVM having a positive in terms of stream fineness compared to IVC-PI-PWM.

Despite the many positives and high performance of STSM-IVC-FMSVM, there are two negatives (low amplitude of the FS (50 Hz) and the presence of fluctuations in the case of a *Ps* that takes large values) that limit the use of this STSM-IVC-FMSVM. These drawbacks are because STSM-IVC-FMSVM is related to the MM of a system. Therefore, these shortcomings will be rectified in future work to enhance the current quality and *Ps*; STSM-IVC-FMSVM will be improved using another technique, such as fractional calculus, NNs approach, and terminal sliding surfaces.

Conclusions

In the domain of WE, the STSM approach is of interest to enhance the characteristics of the DFIG-based CRWT system.

The STSM algorithm is used for the stator powers independent control of the DFIG-CRWT systems using a proposed five-level FSVPWM technique, where the performance was verified using simulation (MATLAB) and experimental work (HIL test).

After modelling the PS, four regulators were developed using STSM regulators (two for the *Ps* and two for the *Qs*).

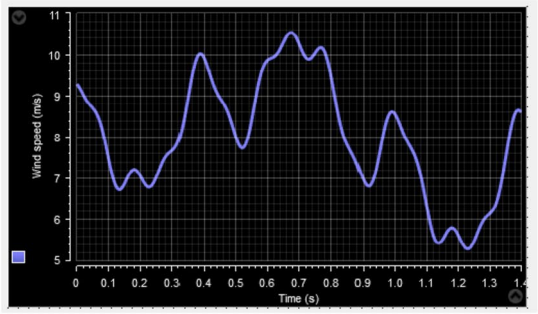

a)WS profile.

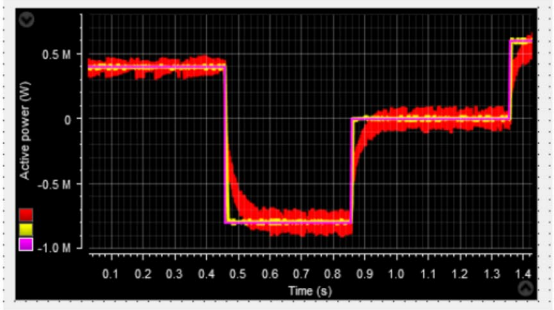

b)*Ps*.

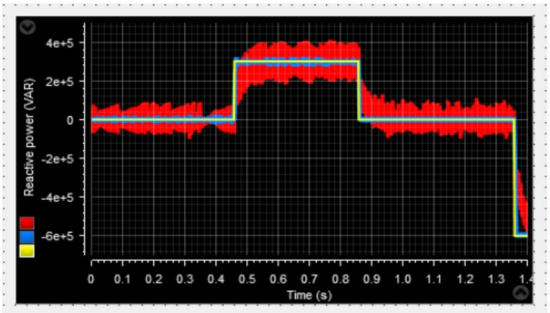

c)*Qs*.

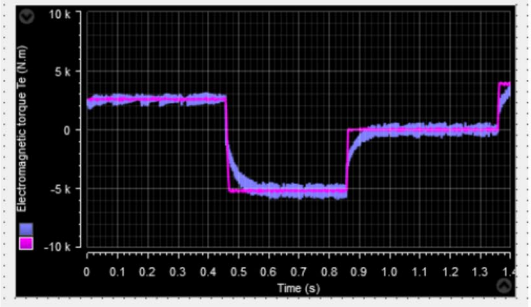

d)Torque

Fig. 15. Experimental results without MPPT technique.

With the appropriate choice of the parameter control, the obtained numerical simulation results are interesting for the CRWT application to ensure robustness and better fineness of the produced energy when the speed is varying. Furthermore, this regulation presents a robust control scheme that has the positive of being easily implantable in calculators.

The simulation shows that the designed nonlinear IVC approach based on the STSM controller and proposed intelligent FMSVM is more robust and performant than IVC-PI (see Tables 6 and 9) and other control schemes (see Table 10). STSM-IVC-FMSVM reduced the THD compared to IVC-PI and other controls.

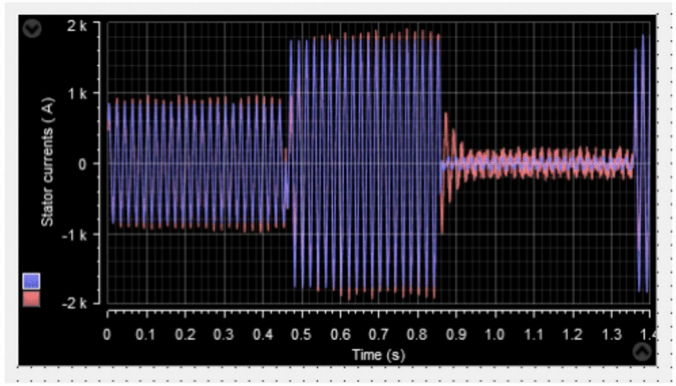

e)Stator current

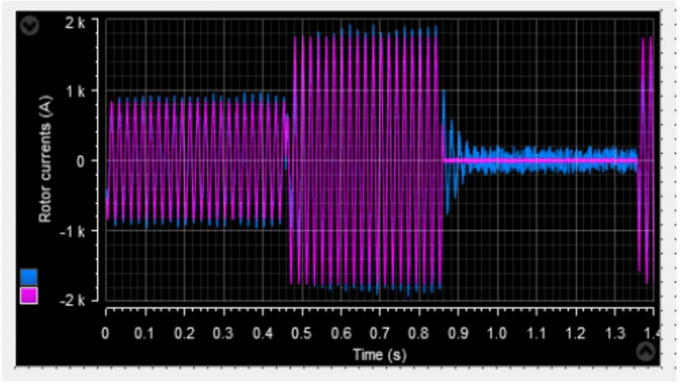

f)Rotor current

Figure 15. (continued)

STSM-IVC-FMSVM gives minimum TRs compared to DPC, NSOSMC, and IVC-PI techniques. All this is evident through the high ratios, as it was found that these ratios in the first test were estimated at 98%, 97%, 93%, and 97% for current, *Qs*, torque and *Ps*, respectively compared to the IVC-PI. In the second test, the percentages were about 95.2%, 98.5%, 97.6%, and 95% for torque, *Qs*, *Ps,* and stream, respectively compared to the IVC-PI.

Summarizing, the main findings of this research are as follows:

- A novel five-level FMSVM to minimize the current THD was presented and confirmed with simulation.
- A novel IVC based on the STSM and the designed five-level FMSVM was confirmed and presented with simulation.
- The robustness of STSM-IVC-FMSVM is presented.
- The performance of STSM-IVC-FMSVM is analyzed, showing that the fluctuations of the stream, *Qs*, electromagnetic torque, and *Ps* are reduced.

The experimental results obtained from the simulation results have proven correct to a large extent, as it is noted from the experimental work that STSM-IVC-FMSVM has a very fast DR compared to IVC-PI. Also, STSM-IVC-FMSVM significantly reduced energy, torque, and current fluctuations compared to IVC-PI.

Despite the many positives and high performance of STSM-IVC-FMSVM, there are two negatives (Low amplitude of the FS (50 Hz) and the presence of fluctuations in the case of a *Ps* that takes large values) that limit the use of this STSM-IVC-FMSVM. These drawbacks are because STSM-IVC-FMSVM is related to the MM of a system. Therefore, these shortcomings will be rectified in future work to enhance the current quality and *Ps*; STSM-IVC-FMSVM will be improved using another technique, such as fractional calculus, NNs approach, and terminal sliding surfaces.

Data availability

The datasets used and/or analysed during the current study available from the corresponding author on reasonable request. In the event of communication, the fist author (Habib Benbouhenni, E-mail: habib.benbouhenni@enp-oran.dz) will respond to any inquiry or request.

Received: 18 December 2024; Accepted: 17 February 2025
Published online: 01 March 2025

References

1. Ruhi, Z. C., Korhan, K., Nurkhat, Z., Abdulkader, H. & Ilhami, C. A review of hybrid renewable energy systems and MPPT methods. *Int. J. Smart Grid.* **6**(3), 72–82 (2022).
2. Ahmed, S. A., Al Lamki, H., Abdulhakim, A. & Hussein, A. K. Techno economic design and analysis of a hybrid renewable energy system for Jazirat Al Halaniyat in Oman. *Int. J. Renew. Energy Res. IJRER* **13**(3), 1039–1050. https://doi.org/10.20508/ijrer.v13i3.13679.g8778 (2024).
3. Djabeur Mohamed, S. Z. et al. Optimized controller design for renewable energy systems by using deep reinforcement learning technique. *Int. J. Renew. Energy Res. IJRER* **14**(1), 101–110. https://doi.org/10.20508/ijrer.v14i1.14362.g8854 (2024).
4. Ghandehari, R., Ali, M. & Alireza Davari, S. A new control algorithm method based on DPC to improve power quality of DFIG in unbalance grid voltage conditions. *Int. J. Renew. Energy Res. IJRER* **8**(4), 2228–2238. https://doi.org/10.20508/ijrer.v8i4.8583.g7527 (2018).
5. Chakib, M., Tamou, N. & Ahmed, E. Contribution of variable speed wind turbine generator based on DFIG using ADRC and RST controllers to frequency regulation. *Int. J. Renew. Energy Res. IJRER* **11**(1), 320–331. https://doi.org/10.20508/ijrer.v11i1.11762.g8136 (2021).
6. Sahar, A. N. et al. Optimal power management and control of hybrid photovoltaic-battery for grid-connected doubly-fed induction generator based wind energy conversion system. *Int. J. Renew. Energy Res. IJRER* **12**(1), 408–421. https://doi.org/10.20508/ijrer.v12i1.12770.g8422 (2022).
7. Kenneth, O. A variable speed wind turbine flywheel based coordinated control system for enhancing grid frequency dynamics. *Int. J. Smart Grid-Ijsmartgrid* **2**(2), 123–134. https://doi.org/10.20508/ijsmartgrid.v2i2.22.g158 (2018).
8. Ngoc, A. V. & Ngoc, S. P. An analytical methodology for aerodynamic analysis of vertical axis wind turbine. *Int. J. Renew. Energy Res. IJRER* **10**(3), 1145–1153. https://doi.org/10.20508/ijrer.v10i3.11001.g7988 (2020).
9. Supreeth, R., Arokkiaswamy, A., Nagarjun Raikar, J. & Prajwal, H. P. Experimental investigation of performance of a small scale horizontal axis wind turbine rotor blade. *Int. J. Renew. Energy Res. IJRER* **9**(4), 1983–1994. https://doi.org/10.20508/ijrer.v9i4.9898.g7804 (2019).
10. Amira, E., Amr, I., Abdellatif, A. & Shaaban, S. Aerodynamic performance and structural design of 5 MW multi rotor system (MRS) wind turbines. *Int. J. Renew. Energy Res. IJRER* **12**(3), 1495–1505. https://doi.org/10.20508/ijrer.v12i3.13343.g8535 (2022).
11. Ercan, E., Selim, S. & Fevzi, C. B. Analysis model of a small scale counter-rotating dual rotor wind turbine with double rotational generator armature. *Int. J. Renew. Energy Res. IJRER* **8**(4), 1849–1858. https://doi.org/10.20508/ijrer.v8i4.8235.g7549 (2018).
12. Faisal, R. B., Subrata, K. S. & Sajal, K. D. Transient stabilization improvement of induction generator based power system using robust integral linear quadratic Gaussian approach. *Int. J. Smart Grid-Ijsmartgrid* **3**(2), 73–83. https://doi.org/10.20508/ijsmartgrid.v3i2.60.g48 (2019).
13. Moez, A., Sahbi, A., Habib, B. Z. & Mohamed, C. A novel fuzzy control strategy for maximum power point tracking of wind energy conversion system. *Int. J. Smart Grid-Ijsmartgrid* **3**(3), 120–127. https://doi.org/10.20508/ijsmartgrid.v3i3.63.g58 (2019).
14. Hüseyin, C., Ahmet, D. & Yuksel, O. Investigation of dynamic behavior of double feed induction generator and permanent magnet synchronous generator wind turbines in failure conditions. *Int. J. Renew. Energy Res. IJRER* **11**(2), 721–729 (2021).
15. Rami Reddy, C. H., Naresh, K., Umapathi Reddy, P. & Sujatha, P. Control of DFIG based wind turbine with hybrid controllers. *Int. J. Renew. Energy Res. IJRER* **10**(3), 1488–1500. https://doi.org/10.20508/ijrer.v10i3.11010.g8028 (2020).
16. Zahra, R., Mansour, R. & Mohammadreza, A. A new control strategy based on reference values changing for enhancing LVRT capability of DFIG in wind farm. *Int. J. Renew. Energy Res. IJRER* **9**(4), 1626–1637. https://doi.org/10.20508/ijrer.v9i4.9952.g7765 (2019).
17. Seyed, M. T., Mohammad, A. P. & Mohammad, R. Z. Comparison between Different DPC Methods Applied to DFIG Wind Turbines. *Int. J. Renew. Energy Res. IJRER* **3**(2), 446–452. https://doi.org/10.20508/ijrer.v3i2.680.g6162 (2023).
18. Resul, C., Ruhi, Z. C. & Korhan, K. Energy management based on supertwisting sliding mode in the standalone photovoltaic power system with battery backup. *Int. J. Smart Grid-Ijsmartgrid* **8**(4), 191–198. https://doi.org/10.20508/ijsmartgrid.v8i4.362.g369 (2024).
19. Youcef, B. & Djilani, B. A. Comparison Study Between SVM and PWM Inverter in Sliding Mode Control of Active and Reactive Power Control of a DFIG for Variable Speed Wind Energy. *Int. J. Renew. Energy Res. IJRER* **2**(3), 471–476. https://doi.org/10.20508/ijrer.v2i3.269.g6047 (2012).
20. Khedher, A., Nihel, K. & Mohamed, F. M. Wind energy conversion system using DFIG controlled by backstepping and sliding mode strategies. *Int. J. Renew. Energy Res. IJRER* **2**(3), 421–434. https://doi.org/10.20508/ijrer.v2i3.249.g6040 (2012).
21. Loubna, B., Khafallah, M., Voyer, D., Mesbahi, A. & Bouragba, T. Nonlinear control based on fuzzy logic for a wind energy conversion system connected to the grid. *Int. J. Renew. Energy Res. IJRER* **10**(1), 193–204. https://doi.org/10.20508/ijrer.v10i1.10381.g7855 (2020).
22. Mohamed, N., Ahmed, E. & Tamou, N. Comparative analysis between PI & backstepping control strategies of DFIG driven by wind turbine. *Int. J. Renew. Energy Res. IJRER* **7**(3), 1307–1316. https://doi.org/10.20508/ijrer.v7i3.6066.g7163 (2017).
23. Mehta, M. & Bhinal, M. Modified rotor flux estimated direct torque control for double fed induction generator. *Int. J. Renew. Energy Res. IJRER* **12**(1), 124–133. https://doi.org/10.20508/ijrer.v12i1.12615.g8380 (2022).
24. Rajendran, S., Jena, D., Diaz, M. & Rodríguez, J. Terminal integral synergetic control for wind turbine at region II using a two-mass model. *Processes* **11**, 616. https://doi.org/10.3390/pr11020616 (2023).
25. Farida, M., Sebti, B. & Ilhami, C. DPC- SVM of DFIG using fuzzy second order sliding mode approach. *Int. J. Smart Grid.* **5**(4), 174–182. https://doi.org/10.20508/ijsmartgrid.v5i4.219.g178 (2021).
26. Leulmi, R., Lekhchine, S. & Medoued, A. Fuzzy logic controller-based power control of DFIG based on wind energy systems. *Int. J. Smart Grid-Ijsmartgrid* **8**(1), 74–80. https://doi.org/10.20508/ijsmartgrid.v8i1.334.g346 (2024).
27. Sumanth, Y., Lakshminarasimman, L. & Rao, G. S. Optimal design of FoPID controller for DFIG based wind energy conversion system using Grey-Wolf optimization algorithm. *Int. J. Renew. Energy Res. IJRER* **12**(4), 2111–2120. https://doi.org/10.20508/ijrer.v12i4.13446.g8594 (2022).
28. Hong Viet, P. N., Van, T. N. & Van, H. N. A combined strategy to improve operational efficiency of microgrids with high integration of solar and wind energy. *Int. J. Renew. Energy Res. IJRER* **13**(3), 1247–1258. https://doi.org/10.20508/ijrer.v13i3.14194.g8797 (2024).
29. Boris, D., Bane, P., Dragan, M., Vladimir, K. & Djura, O. Artificial intelligence based vector control of induction generator without speed sensor for use in wind energy conversion system. *Int. J. Renew. Energy Res. IJRER* **5**(1), 299–307. https://doi.org/10.20508/ijrer.v5i1.2030.g6498 (2015).
30. Mahersi, E. E., Kheder, A. & Mohamed, F. M. The wind energy conversion system using PMSG controlled by vector control and SMC strategies. *Int. J. Renew. Energy Res. IJRER* **3**(1), 41–50. https://doi.org/10.20508/ijrer.v3i1.419.g6084 (2013).
31. Mohammed, F., Ahmed, E. & Tamou, N. Comparative analysis between robust SMC & conventional PI controllers used in WECS based on DFIG. *Int. J. Renew. Energy Res. IJRER* **7**(4), 2151–2161. https://doi.org/10.20508/ijrer.v7i4.6441.g7267 (2017).
32. Qiu, X., Wang, W., Yang, J., Jiang, J. & Yang, J. Phase-inductance-based position estimation method for interior permanent magnet synchronous motors. *Energies* **10**, 2002. https://doi.org/10.3390/en10122002 (2017).
33. Brando, G., Dannier, A. & Spina, I. Performance analysis of a full order sensorless control adaptive observer for doubly-fed induction generator in grid connected operation. *Energies* **14**, 1254. https://doi.org/10.3390/en14051254 (2021).
34. Marwa, G., Jihen, A.-Z. & Mohamed, W. N. Modelling of a PMSG based wind turbine system with diode rectifier based generator side converter. *Int. J. Renew. Energy Res. IJRER* **12**(3), 1532–1539. https://doi.org/10.20508/ijrer.v12i3.13044.g8538 (2022).

35. Caruso, M. et al. A general and accurate measurement procedure for the detection of power losses variations in permanent magnet synchronous motor drives. *Energies* **13**, 5770. https://doi.org/10.3390/en13215770 (2020).
36. Sumega, M., Rafajdus, P. & Stulrajter, M. Current harmonics controller for reduction of acoustic noise, vibrations and torque ripple caused by cogging torque in PM motors under FOC operation. *Energies* **13**, 2534. https://doi.org/10.3390/en13102534 (2020).
37. Wang, Q., Yu, H., Wang, M. & Qi, X. A novel adaptive neuro-control approach for permanent magnet synchronous motor speed control. *Energies* **11**, 2355. https://doi.org/10.3390/en11092355 (2018).
38. Ahmed, M. Comparative study between direct and indirect vector control applied to a wind turbine equipped with a double-fed asynchronous machine article. *Int. J. Renew. Energy Res. IJRER* **3**(1), 88–93. https://doi.org/10.20508/ijrer.v3i1.465.g6109 (2013).
39. Chetouani, E., Errami, Y., Obbadi, A. & Sahnoun, S. Backstepping and indirect vector control for rotor side converter of doubly fed-induction generator with maximum power point tracking. In *Digital Technologies and Applications. ICDTA 2021. Lecture Notes in Networks and Systems* Vol. 211 (eds Motahhir, S. & Bossoufi, B.) (Springer, 2021). https://doi.org/10.1007/978-3-030-73882-2_155.
40. Wang, F., Zhang, Z., Mei, X., Rodríguez, J. & Kennel, R. Advanced control strategies of induction machine: Field oriented control, direct torque control and model predictive control. *Energies* **11**, 120. https://doi.org/10.3390/en11010120 (2018).
41. Amrane, F., Chaiba, A., Babas, B. E. & Mekhilef, S. Design and implementation of high performance field oriented control for grid-connected doubly fed induction generator via hysteresis rotor current controller. *Rev. Sci. Techni.- Electrotechn. Et Energy* **61**(4), 319–324 (2016).
42. Amrane, F. & Chaiba, A. A novel direct power control for grid-connected doubly fed induction generator based on hybrid artificial intelligent control with space vector modulation. *Rev. Sci. Techni.- Electrotechn. Et Energy* **61**(3), 263–268 (2016).
43. Fayssal, A., Bruno, F., Azeddine, C. Experimental investigation of efficient and simple wind-turbine based on DFIG-direct power control using LCL-filter for stand-alone mode. *ISA Trans*. In Press, 1–34. https://doi.org/10.1016/j.isatra.2021.07.008 (2021).
44. Samir, M., Mohamed, H., Nadir, K. & Selman, K. Neural network based field oriented control for doubly-fed induction generator. *Int. J. Smart Grid-Ijsmartgrid* **2**(3), 183–187. https://doi.org/10.20508/ijsmartgrid.v2i3.18.g18 (2018).
45. Yahdou, A., Djilali, A. B., Boudjema, Z. & Mehedi, F. Improved vector control of a counter-rotating wind turbine system using adaptive backstepping sliding mode. *J. Européen des Systèmes Automatisés* **53**(5), 645–651 (2020).
46. Ruhi, Z. C., Korhan, K., Mariacristina, R., Abdelhakim, B. & Abdelfatah, N. A comparative analysis of P&O, IC and supertwisting sliding mode based MPPT methods for PV and fuel cell sourced hybrid system. *Int. J. Renew. Energy Res. IJRER* **13**(3), 1431–1442. https://doi.org/10.20508/ijrer.v13i3.14550.g8815 (2023).
47. Abdellah, Z. & Ahmed, A. Fuzzy-super twisting sliding mode MPPT control for three-phase grid-connected PV. *Int. J. Renew. Energy Res. IJRER* **8**(4), 1812–1823. https://doi.org/10.20508/ijrer.v8i4.8062.g7487 (2018).
48. Yaichi, I., Semmah, A., Wira, P. & Djeriri, Y. Super-twisting sliding mode control of a doubly-fed induction generator based on the SVM strategy. *Period. Polytechn. Electr. Eng. Comput. Sci.* **63**(3), 178–190. https://doi.org/10.3311/PPee.13726 (2019).
49. Orhan, K. & Ferhat, B. Super twisting algorithm based sliding mode controller for buck converter feeding constant power load. *Int. J. Renew. Energy Res. IJRER* **12**(1), 134–145. https://doi.org/10.20508/ijrer.v12i1.12448.g8383 (2022).
50. Zeb, K. et al. Design of super twisting sliding mode controller for a three-phase grid-connected photovoltaic system under normal and abnormal conditions. *Energies* **13**, 3773. https://doi.org/10.3390/en13153773 (2020).
51. Gao, P., Zhang, G. & Lv, X. Model-free control using improved smoothing extended state observer and super-twisting nonlinear sliding mode control for PMSM drives. *Energies* **14**, 922. https://doi.org/10.3390/en14040922 (2021).
52. Valenzuela, F. A., Ramírez, R., Martínez, F., Morfín, O. A. & Castañeda, C. E. Super-twisting algorithm applied to velocity control of DC motor without mechanical sensors dependence. *Energies* **13**, 6041. https://doi.org/10.3390/en13226041 (2020).
53. Liu, Y., Fang, J., Tan, K., Huang, B. & He, W. Sliding mode observer with adaptive parameter estimation for sensorless control of IPMSM. *Energies* **13**, 5991. https://doi.org/10.3390/en13225991 (2020).
54. Ibrahim, Y., Semmah, A. & Patrice, W. Neuro-second order sliding mode control of a DFIG based wind turbine system. *J. Electr. Electron. Eng.* **13**(1), 63–68 (2020).
55. Listwan, J. Application of super-twisting sliding mode controllers in direct field-oriented control system of six-phase induction motor: Experimental studies. *Power Electron. Drives* **3**(1), 23–34. https://doi.org/10.2478/pead-2018-0013 (2018).
56. Alhato, M. M., Ibrahim, M. N., Rezk, H. & Bouallègue, S. An enhanced DC-link voltage response for wind-driven doubly fed induction generator using adaptive fuzzy extended state observer and sliding mode control. *Mathematics* **9**, 963. https://doi.org/10.3390/math9090963 (2021).
57. Mazen Alhato, M., Bouallègue, S. & Rezk, H. Modeling and performance improvement of direct power control of doubly-fed induction generator based wind turbine through second-order sliding mode control approach. *Mathematics* **8**, 2012. https://doi.org/10.3390/math8112012 (2020).
58. Han, Y. & Ma, R. Adaptive-gain second-order sliding mode direct power control for wind-turbine-driven DFIG under balanced and unbalanced grid voltage. *Energies* **12**, 3886. https://doi.org/10.3390/en12203886 (2019).
59. Saihi, L., Bakou, Y., Harrouz, A., Boura, M., Colak, I., Kayisli, K. Fuzzy-sliding mode control second order of wind turbine based on DFIG. in *2022 10th International Conference on Smart Grid (icSmartGrid), Istanbul, Turkey*. 296–300. https://doi.org/10.1109/icSmartGrid55722.2022.9848587 (2022).
60. Farida, M., Belkacem, S., Colak, I. Fuzzy high order sliding mode control based DPC of DFIG using SVM. in *2021 9th International Conference on Smart Grid (icSmartGrid), Setubal, Portugal*. 278–282. https://doi.org/10.1109/icSmartGrid52357.2021.9551262 (2021).
61. El Qouarti, O., Essadki, A., Laghridat, H., Nasser, T. Power control of DFIG based WECS using SOSMC and PSO algorithm. in *2022 2nd International Conference on Innovative Research in Applied Science, Engineering and Technology (IRASET), Meknes, Morocco*. 1–6. https://doi.org/10.1109/IRASET52964.2022.9738382 (2022).
62. Djilali, L., Badillo-Olvera, A., Yuliana Rios, Y., López-Beltrán, H. & Saihi, L. Neural high order sliding mode control for doubly fed induction generator based wind turbines. *IEEE Latin Am. Trans.* **20**(2), 223–232. https://doi.org/10.1109/TLA.2022.9661461 (2022).
63. Xinyi, L., Laghrouche, S., Harmouche, M., Fellag, R., Wack, M. Super twisting sliding mode MPPT control of an IM based wind energy conversion system. in *2015 4th International Conference on Electrical Engineering (ICEE), Boumerdes*, 1–5. https://doi.org/10.1109/INTEE.2015.7416793 (2015).
64. Li, L., Su, Y., Kong, L., Jiang, K. & Zhou, Y. TDE-based adaptive super-twisting multivariable fast terminal slide mode control for cable-driven manipulators with safety constraint of error. *IEEE Access* **11**, 6656–6664. https://doi.org/10.1109/ACCESS.2022.3232555 (2023).
65. Habib, B., Bizon, N., Colak, I., Thounthong, P. & Takorabet, N. Simplified super twisting sliding mode approaches of the double-powered induction generator-based multi-rotor wind turbine system. *Sustainability* **14**, 5014. https://doi.org/10.3390/su14095014 (2022).
66. Belabbas, B., Allaoui, T., Tadjine, M., Mouloud, D. Comparative study of back-stepping controller and super twisting sliding mode controller for indirect power control of wind generator. *Int. J. Syst. Assur. Eng. Manag.* **10**(1). https://doi.org/10.1007/s13198-019-00905-7 (2019).
67. Kamel, D. E., Abdelkader, M., Larbi, B. & Van Den Bossche, A. P. M. A comprehensive review of LVRT capability and sliding mode control of grid-connected wind-turbine-driven doubly fed induction generator. *Automatika* **57**(4), 922–935. https://doi.org/10.7305/automatika.2017.05.1813 (2016).

68. Lat Leily, M.R., Tohidi, S., Hashemzadeh, F., Shotorbani, A.M. Novel sliding mode controller for power control of a doubly fed induction generator in variable speed wind turbine. in *2019 Iranian Conference on Renewable Energy & Distributed Generation (ICREDG), Tehran, Iran*, 1–6. https://doi.org/10.1109/ICREDG47187.2019.194147 (2019).
69. Salas-Peña, O., Herman, C. & de León-Morales, J. Robust adaptive control for a DC servomotor with wide backlash nonlinearity. *Automatika* **56**(4), 436–442. https://doi.org/10.1080/00051144.2015.11828657 (2015).
70. Nicolás, G., Salas-Peña, O., de León-Morales, J., Sergio, R. & Parra-Vega, V. Observer-based integral sliding mode approach for bilateral teleoperation with unknown time delay. *Automatika* **57**(3), 749–760. https://doi.org/10.7305/automatika.2017.02.1399 (2016).
71. Hamza, G. et al. Fractional order proportional integral super-twisting sliding mode controller for wind energy conversion system equipped with doubly fed induction generator. *J. Power Electron.* **22**(8), 1357–1357. https://doi.org/10.1007/s43236-022-00430-0 (2022).
72. Mansoor, A. S., Zubair, A. M., Mahesh, K. & Mazhar, H. B. Wind energy integration: Dynamic modeling and control of DFIG based on super twisting fractional order terminal sliding mode controller. *Energy Rep.* **7**, 6031–6043. https://doi.org/10.1016/j.egyr.2021.09.022 (2021).
73. Ravikiran, H. & Tukaram, M. Modified super twisting algorithm based sliding mode control for LVRT enhancement of DFIG driven wind system. *Energy Rep.* **8**, 3600–3613. https://doi.org/10.1016/j.egyr.2022.02.235 (2022).
74. Beik, O. & Al-Adsani, A. S. Active and passive control of a dual rotor wind turbine generator for DC grids. *IEEE Access* **9**, 1987–1995. https://doi.org/10.1109/ACCESS.2020.3047267 (2021).
75. Luo, X. & Niu, S. A novel contra-rotating power split transmission system for wind power generation and its dual MPPT control strategy. *IEEE Trans. Power Electron.* **32**(9), 6924–6935. https://doi.org/10.1109/TPEL.2016.2629021 (2017).
76. Zhao, Y., Teng, D., Li, D. & Zhao, X. Comparative research on four-phase dual armature-winding wound-field doubly salient generator with distributed field magnetomotive forces for high-reliability application. *IEEE Access* **9**, 12579–12591. https://doi.org/10.1109/ACCESS.2021.3051310 (2021).
77. Zhao, W., Lipo, T. A. & Kwon, B. A novel dual-rotor, axial field, fault-tolerant flux-switching permanent magnet machine with high-torque performance. *IEEE Trans. Magn.* **51**(11), 1–4. https://doi.org/10.1109/TMAG.2015.2445926 (2015).
78. Fukami, T., Momiyama, M., Shima, K., Hanaoka, R. & Takata, S. Steady-state analysis of a dual-winding reluctance generator with a multiple-barrier rotor. *IEEE Trans. Energy Convers.* **23**(2), 492–498. https://doi.org/10.1109/TEC.2008.918656 (2008).
79. Tarek, B., Islam, A. S. & Doaa Khalil, I. Performance enhancement of doubly-fed induction generator-based-wind energy system. *Int. J. Renew. Energy Res. IJRER* **13**(1), 311–325. https://doi.org/10.20508/ijrer.v13i1.13649.g8685 (2023).
80. Shen, X. et al. A High-gain observer-based adaptive super-twisting algorithm for DC-link voltage control of NPC converters. *Energies* **13**, 1110. https://doi.org/10.3390/en13051110 (2020).
81. Chen, S., Zhang, X., Wu, X., Tan, G. & Chen, X. Sensorless control for IPMSM based on adaptive super-twisting sliding-mode observer and improved phase-locked loop. *Energies* **12**, 1225. https://doi.org/10.3390/en12071225 (2019).
82. Uddin, W. et al. Control of output and circulating current of modular multilevel converter using a sliding mode approach. *Energies* **12**, 4084. https://doi.org/10.3390/en12214084 (2019).
83. Habib, B., Boudjema, Z. & Belaidi, A. Indirect vector control of a DFIG supplied by a two-level FSVM inverter for wind turbine system. *Majlesi J. Electr. Eng.* **13**(1), 45–54 (2019).
84. Habib, B., Bizon, N. & Colak, I. A brief review of space vector modulation (SVM) methods and a new SVM technique based on the minimum and maximum of the three-phase voltages. *Iran. J. Electr. Electron. Eng.* **18**(3), 1–18. https://doi.org/10.22068/IJEEE.18.3.2358 (2022).
85. Ayrira, W., Ourahoua, M., El Hassounia, B. & Haddib, A. Direct torque control improvement of a variable speed DFIG based on a fuzzy inference system. *Math. Comput. Simul.* **167**, 308–324. https://doi.org/10.1016/j.matcom.2018.05.014 (2020).
86. Quan, Y., Hang, L., He, Y. & Zhang, Y. Multi-resonant-based sliding mode control of DFIG-based wind system under unbalanced and harmonic network conditions. *Appl. Sci.* **9**, 1124. https://doi.org/10.3390/app9061124 (2019).
87. Alami, H. E. et al. FPGA in the loop implementation for observer sliding mode control of DFIG-generators for wind turbines. *Electronics* **11**(1), 116. https://doi.org/10.3390/electronics11010116 (2022).
88. Echiheb, F. et al. Robust sliding-backstepping mode control of a wind system based on the DFIG generator. *Sci. Rep.* **12**, 11782. https://doi.org/10.1038/s41598-022-15960-7 (2022).
89. Benbouhenni, H. et al. Hardware-in-the-loop simulation to validate the fractional-order neuro-fuzzy power control of variable-speed dual-rotor wind turbine systems. *Energy Rep.* **11**, 4904–4923. https://doi.org/10.1016/j.egyr.2024.04.049 (2024).
90. Adil, Y. et al. Application of backstepping control with nonsingular terminal sliding mode surface technique to improve the robustness of stator power control of asynchronous generator-based multi-rotor wind turbine system. *Electr. Power Compon. Syst.* https://doi.org/10.1080/15325008.2024.2304688 (2024)
91. Hamza, G. et al. A new scheme of the fractional-order super twisting algorithm for asynchronous generator-based wind turbine. *Energy Rep.* **9**, 6311–6327. https://doi.org/10.1016/j.egyr.2023.05.267 (2023).
92. Habib, B., Hamza, G., Ilhami, C., Nicu, B. & Phatiphat, T. Synergetic-PI controller based on genetic algorithm for DPC-PWM strategy of a multi-rotor wind power system. *Sci. Rep.* **13**, 13570. https://doi.org/10.1038/s41598-023-40870-7 (2023).
93. Habib, B., Bizon, N., Colak, I. Super-twisting hysteresis controller for multi-rotor wind energy systems. Int. J. Electron. 1–20. https://doi.org/10.1080/00207217.2024.2312086 (2024).
94. Habib, B., Elhadj, B., Hamza, G., Nicu, B. & Ilhami, C. A new PD(1+PI) direct power controller for the variable-speed multi-rotor wind power system driven doubly-fed asynchronous generator. *Energy Rep.* **8**, 15584–15594. https://doi.org/10.1016/j.egyr.2022.11.136 (2022).
95. Habib, B., Dalal, Z., Nicu, B. & Ilhami, C. A new PI(1 +PI) controller to mitigate power ripples of a variable-speed du-al-rotor wind power system using direct power control. *Energy Rep.* **10**, 3580–3598. https://doi.org/10.1016/j.egyr.2023.10.007 (2023).
96. Yessef, M. et al. Real-time validation of intelligent super twisting sliding mode control for variable-speed DFIG using dSPACE 1104 board. *IEEE Access* **12**, 31892–31915. https://doi.org/10.1109/ACCESS.2024.3367828 (2024).
97. Younes, S. et al. New intelligent direct power control of DFIG-based wind conversion system by using machine learning under variations of all operating and compensation modes. *Energy Rep.* **7**, 6394–6412. https://doi.org/10.1016/j.egyr.2021.09.075 (2021).
98. Benbouhenni, H., Nicu, B., Ilhami, C., Mohamed, I. M. & Mourad, Y. Direct active and reactive powers control of double-powered asynchronous generators in multi-rotor wind power systems using modified synergetic control. *Energy Rep.* **10**, 4286–4301. https://doi.org/10.1016/j.egyr.2023.10.085 (2023).

Acknowledgements

This research was supported by King Khalid University, Research Project RGP.1/251/45.

Author contributions

Conceptualization:Habib Benbouhenni, Nicu Bizon, Z.M.S. Elbarbary, Ilhami Colak methodology:Habib Benbouhenni, Nicu Bizon, Z.M.S. Elbarbary, Ilhami Colak, Mohammed M. Alammer software:Habib Benbouhenni, Nicu Bizon, Mourad Yessef validation:Habib Benbouhenni, Nicu Bizon, Mourad Yessef formal analysis:Habib Benbouhenni, Nicu Bizon, Z.M.S. Elbarbary, Ilhami Colak, Mohammed M. Alammer investigation:Habib

Benbouhenni, Mourad Yessef, Badre Bossoufi, Z.M.S. Elbarbary resources:Habib Benbouhenni, Nicu Bizon, Z.M.S. Elbarbary data curation:Habib Benbouhenni, Nicu Bizon, Z.M.S. Elbarbary, Ilhami Colak writing—original draft preparation:Habib Benbouhenni, Nicu Bizon, Z.M.S. Elbarbary, Ilhami Colak, Mohammed M. Alammer writing—review and editing:Habib Benbouhenni, Nicu Bizon, Z.M.S. Elbarbary, Mohammed M. Alammer visualization:Habib Benbouhenni, Nicu Bizon, Mourad Yessef, Z.M.S. Elbarbary, Ilhami Colak, Mohammed M. Alammer supervision:Habib Benbouhenni, Nicu Bizon, Mourad Yessef, Badre Bossoufi, Z.M.S. Elbarbary, Ilhami Colak, Mohammed M. Alammer project administration:Habib Benbouhenni, Nicu Bizon, Z.M.S. Elbarbary, Ilhami Colak, Mohammed M. Alammer funding acquisition:Habib Benbouhenni, Nicu Bizon, Z.M.S. Elbarbary, Ilhami Colak, Mohammed M. Alammer All authors have read and agreed to the published version of the manuscript. .

Funding
Not applicable.

Declarations

Competing interests
The authors declare no competing interests.

Additional information
Correspondence and requests for materials should be addressed to H.B.

Reprints and permissions information is available at www.nature.com/reprints.

Publisher's note Springer Nature remains neutral with regard to jurisdictional claims in published maps and institutional affiliations.